REPORT METEOROLOGY AND CLIMATOLOGY No. 118, 2021

SMHI Gridded Climatology

Sandra Andersson, Lars Bärring, Tomas Landelius, Patrick Samuelsson, Semjon Schimanke

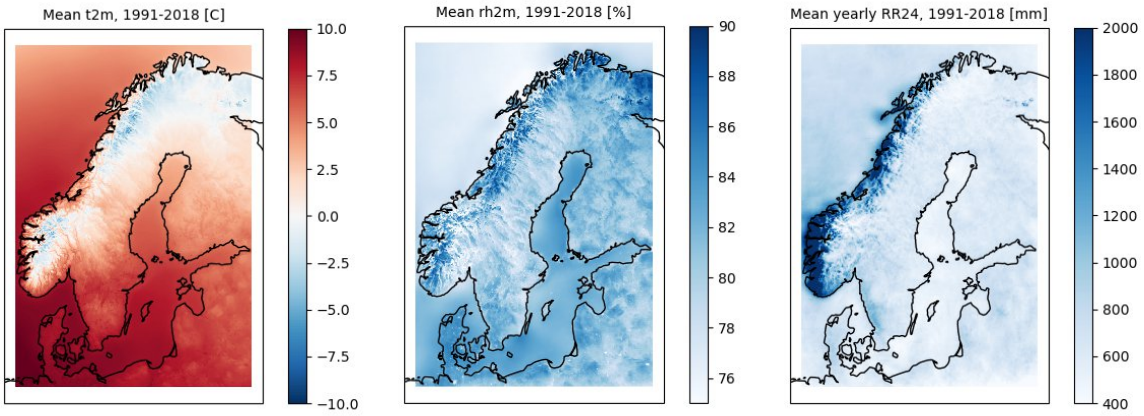

Skriv text här

Front:
Maps illustrating data for the time period 1991-2018 based on SMHI Gridded Climatology. Left: hourly mean T2m. Middle: Hourly rh2m. Right: Yearly mean RR.

ISSN: 0347-2116

REPORT METEOROLOGY AND CLIMATOLOGY No. 118, 2021

SMHI Gridded Climatology

Sandra Andersson, Lars Bärring, Tomas Landelius, Patrick Samuelsson, Semjon Schimanke

Reviewer: Erik Engström
Department: Information and Statistics

Empty page

Summary

A gridded dataset (SMHI Gridded Climatology - SMHIGridClim) has been produced for the years 1961 - 2018 over an area covering the Nordic countries on a grid with 2.5 km horizontal resolution. The variables considered are the two meter temperature and two meter relative humidity on 1, 3 or 6 hour resolution, varying over the time period covered, the daily minimum and maximum temperatures, the daily precipitation and the daily snow depth. The gridding was done using optimal interpolation with the gridpp open source software from the Norwegian Meteorological Institute.

Observations for the analysis are provided by the Swedish, Finish and Norwegian meteorological institutes, and the ECMWF. The ECA&D observation data set (e.g. used for the gridded E-OBS dataset) was considered for inclusion but was left out because of complications with time stamps and accumulation periods varying between countries and periods. Quality check of the observations was performed using the open source software TITAN, also developed at the Norwegian Meteorological Institute.

The first guess to the optimal interpolation was given by statistically downscaled forecasts from the UERRA-HARMONIE reanalysis at 11 km horizontal resolution. The downscaling was done to fit the output from the operational MEPS NWP system at 2.5 km with a daily and yearly variation in the downscaling parameters.

The quality of the SMHIGridClim dataset, in terms of annual mean RMSE, was shown to be similar to that of gridded datasets covering the other Nordic countries; "seNorge" from Norway and the dataset "FMI_ClimGrid" from Finland.

Sammanfattning

Ett klimatologiskt griddat datasett (SMHI Gridded Climatology - SMHIGridClim) har tagits fram för åren 1961 – 2018. Data täcker de nordiska länderna med en horisontell upplösning av 2,5 km. Variablerna som tagits fram är lufttemperatur och relativ luftfuktighet vid 2m höjd med en upplösning av1,3 eller 6 timmar beroende av tidsperiod, samt dygnsupplöst min- och maxtemperatur, nederbörd och snödjup. Datasetet är framtaget med optimal interpolation av stationsdata genom analysverktyget gridpp, som är en öppet tillgänglig programvara från Norska Meteorologiska Institutet.

Observationer till analysen har erhållits från de svenska, norska och finska meteorologiska instituten, samt ECMWF. En ansats gjordes också att använda observationer från datasetet ECA&D från KNMI, men på grund av svårigheter med att tidsstämplarna för data från olika länder inte överensstämde, uteslöts datasetet ur analysen. Kvalitetskontroll av observationerna gjordes med programvaran TITAN, som även den finns tillgänglig från och utvecklats av Norska Meteorologiska Institutet.

Som en första gissning till interpolationen användes statistiskt nerskalade prognosfält (från 11 km till 2,5 km upplösning) från UERRA-HARMONIE. Nerskalningen gjordes mot fält från den operationella numeriska väderprognosmodellen MEPS. Anpassningen gjordes med nedskalningsparametrar som varierar över året och dygnet.

Kvalitén hos "SMHIGridClim med avseende på genomsnittligt RMSE är liknande den som tagits fram för griddade data för andra nordiska länderna med varierande analysmetoder; "seNorge" från Norge och "FMI_ClimGrid" från Finland.

Empty page

Table of contents

1 Introduction

The SMHI Gridded Climatology was developed to meet the need for a climate reference dataset covering Nordic countries with high resolution, reaching back to 1961. In first place it was designed to be used for the climate scenario service at SMHI, with regards to a reference for historical data and for bias adjustment of model climate scenarios.

A review of available datasets showed that the best candidate as climate reference for Nordic conditions today is the Nordic Gridded Climate Dataset (NGCD) from Met Norway (Lussana et al., 2019). However NGCD does not provide data for the entire period back to 1961, neither does it provide sub daily information about the variables. Another candidate was data from the UERRA surface reanalysis with MESCAN-SURFEX. It provides analyses of daily accumulated precipitation and six-hourly analyses of air temperature and relative humidity. However, analyses are only available at hour 00, 06, 12 and 18. It lacks analysis of Tn, Tx, and Sn and have been shown to have some quality issues with RR.

The methodology used here is based on combining a first guess from reanalysis fields with observations, using the gridpp system which is an open source software from the Norwegian Meteorological Institute. Setting up a surface reanalysis system with gridpp at SMHI also provided a start for a production chain of climate data, where additional parameters can be considered. In addition there are synergies with a system simultaneously being implemented for production of near-realt time climate data. This system is also using gridpp and is the candidate for replacing the current operational system MESAN.

Observations are provided by the Swedish, Finish and Norwegian meteorological institutes, and the European Centre for Medium-Range Weather Forecasts (ECMWF). Quality check of the observations was performed using the TITAN package developed at the Norwegian Meteorological Institute. For reanalysis data, fields from UERRA-HARMONIE with a horizontal resolution of 11 km were downscaled, using forecasts from the Nordic operational NWP system MEPS for an overlapping period, resulting in data fields with a horizontal resolution of 2.5 km for the analysis. An illustration of the processing steps is shown in fig.1.1 below, and are described more in detail in respective section of this documentation.

Variables produced with the system are near-surface air temperature (T2m), near-surface maximum and minimum temperatures (Tx and Tn), precipitation (RR), near-surface relative humidity (Rh2m) and snow depth (Sn).

Data spans the years 1961-2018 as reanalysis fields from UERRA are available for this period of time. The time resolution of temperature and relative humidity data varies over the years, from every 6th hour for the period 1961-1967, every 3rd hour for the period 1968-1996, and every hour for the period 1997-2018, depending on the amount of observational data available. For the remaining parameters, the resolution is daily.

Data are provided for an area covering Sweden, Norway, Finland and the vicinity of the Baltic sea. The quality of the analysis varies over time, as it depends on the quality of the forecasts as well as the quality and density of the observations that are available for the analysis. Besides the actual analysis for a given data, the system also outputs a map with an estimate of the error in the analysis and a list of the observations used together with the values of the first guess, the analysis and the cross validation at each observation point.

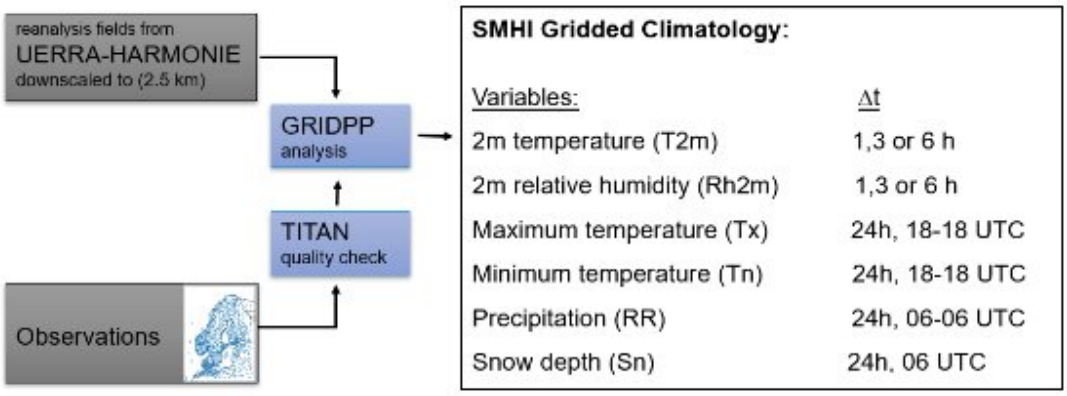

Figure 1.1 Simple overview of the processing steps of data for analysis with gridpp, and the produced variables in SMHIGridClim.

2 Data

For the analysis, observations as well as gridded fields of numerical weather prediction (NWP) data were used for the targeted variables: T2m, Tx, Tn, RR, Rh2m and Sn. However, for the two latter variables, the analysis was not entirely based on data of these entities.

For near-surface humidity conditions the analysis with gridpp was done on near-surface dewpoint temperature (Td2m) instead of relative humidity. The reason for this is that it is more difficult to analyze a variable with hard lower and upper limits as is the case for relative humidity at 0% and 100%. Also snow depth was not available as a parameter from NWP analysis. Instead snow depth had to be derived from the snow water equivalent and snow density.

2.1 Numerical weather prediction data

Forecasts from the UERRA-HARMONIE reanalysis (UERRA, 2020) were used as a starting point for the creation of the first guess fields entering the analysis. It is worth pointing out that the analysis fields from UERRA-HARMONIE (available at 00, 06, 12 and 18 UTC) are not used for the first guess. The reason for this is that these fields already include information from some of the observations that will be used in the present analysis.

The UERRA-HARMONIE fields were complemented with matching forecasts from the Nordic operational NWP system MEPS (Frogner et al., 2019) for the overlapping time period 201601-201907. This combination allowed for a downscaling of the original UERRA-HARMONIE forecasts, at a horizontal resolution of 11 km, to the SMHIGridClim grid, defined as a subset with 823 x 567 (rows x cols) points from the MEPS grid at a horizontal resolution of 2.5 km. The three regions defining the model area of UERRA-HARMONIE, MEPS and SMHIGridClim are shown in Figure 2.1.

UERRA-HARMONIE data was partly available on disk at the National Supercomputer Centre (NSC) at Linköping university at the start of the project, and was then supplemented with additional data from the Meteorological Archival and Retrieval System (MARS) at ECMWF. Table 2.1 lists the forecast cycles and lengths of the UERRA-HARMONIE forecast fields used for the different entities in the SMHIGridClim dataset.

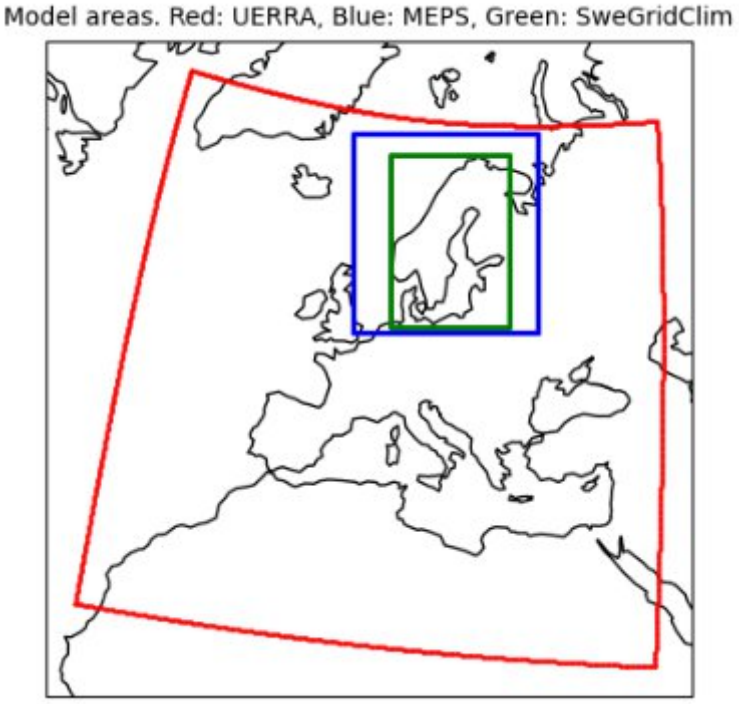

Figure 2.1 The areas covered by the different model grids. Red: UERRA-HARMONIE at 11 km. Blue: MEPS at 2.5 km. Green: SMHIGridClim at 2.5 km (subset of the MEPS grid).

MEPS data was retrieved from the MARS archive at NSC. In this case only 6 hourly forecast data was retrieved for T2m and Td2m, i.e. for 00+06, 06+06, 12+06, and 18+06. No MEPS fields for Tn and Tx were retrieved, instead T2m relations for the midpoint of each Tn/Tx time window were used, see Table 2.1. Snow depth is only measured at 06 UTC so 00+06 forecasts were used. However, Sn was not available as a parameter from UERRA-HARMONIE and MEPS. Instead it had to be derived from the snow water equivalent and snow density. Unfortunately the snow density was not available from the MEPS model so only the snow water equivalent was downscaled. Daily precipitation was derived from a combination of accumulation periods as described in Table 2.1.

Daily minimum and maximum temperatures were derived as point-wise min and max values over the 12 forecast fields in Table 2.1. Note that the last three fields from the 12 UTC cycle relate to the 12 UTC cycle from the previous day. The daily precipitation (06-06 UTC) was calculated as rr24@00+18 - rr24@00+06 + rr24@12+18 - rr24@12+06. Note that the 00 UTC cycle refers to the previous day. The reason for this combination of precipitation forecasts was twofold. First we wanted to avoid moist spin-up problems and hence dismiss the forecasts during the first six hours. Second, the data assimilation at 00 and 12 UTC are supposed to contain more information than other cycles. Since shorter forecasts are supposed to be more reliable than longer ones we did not consider to use the simpler expression rr24@00+30 - rr24@00+06.

Variable	Forecast cycle 00	Forecast cycle 06	Forecast cycle 12	Forecast cycle 18
T2m, Rh2m	00+01 00+02 00+03 00+04 00+05 00+06	06+01 06+02 06+03 06+04 06+05 06+06	12+01 12+02 12+03 12+04 12+05 12+06	18+01 18+02 18+03 18+04 18+05 18+06
Tn/Tx 18-18	00+03-04 00+04-05 00+05-06 00+06-09 00+09-12 00+12-15		12+03-04 12+04-05 12+05-06 12+06-09 12+09-12 12+12-15	
RR 06-06	00+06 00+18		12+06 12+18	
SWE, rho	00+06			

Table 2.1 Forecast cycles and lengths of the UERRA-HARMONIE fields for the different entities in the SMHIGridClim dataset. (SWE: snow water equivalent, rho: snow density)

2.2 National data sets

Local observations were collected from the national meteorological services in Sweden, Norway and Finland. Swedish observations are extracted from SMHI's Meteorological Observational Real-time and Archive (MORA) database. More information (in Swedish) can be found here https://www.smhi.se/data/utforskaren-oppna-data/. Data is quality controlled and more data is added constantly, both by adding real-time observations as well as by adding historical observations through data rescue activities. SMHI has an open data policy so the data is freely available. Data from the Norwegian Meteorological Institute were fetched via with the Frost API (personal communication with Mariken Homleid). Frost is MET Norway's archive of historical weather and climate data and the data is freely available (see https://frost.met.no). Data from the Finnish Meteorological Institute (FMI) were fetched from FMI's internal data base (personal communication with Viivi Kallio-Myers). However, data should be also freely available at https://en.ilmatieteenlaitos.fi/open-data.

It is note worthy that the fetching of the observations from the national data archives was incomplete in the first attempts. Comparisons with BUFR (see section 2.3) and ECA&D data (section 2.4) revealed that data from the national archives were missing from all institutes. Following reasons were discovered for the missing data.

1. At SMHI, the fetching scripts include source code that check if data are available for the specified time. However, unfortunately, the test checked only if T2m was available and did not consider other parameters. So, dates without T2m were neglected even if other parameters as e.g. precipitation were available.

2. At MET No, data was prepared based on a station list including active stations only. For instance, data from stations that are not operational any longer were missed.
3. FMI used bad keywords for latitude and longitude, which were then reported as zero. However, observations without information on the position of the data cannot be used in the system. Another miss was the station height. For some older stations the corresponding information could not be created and consequently the data could not be used for SMHIGridClim.

The lesson learnt here is that the number of observations need to be checked against other sources as much as possible. Beside a fix for the station height for some of the Finish stations, all discovered bugs were solved within a couple of days.

For near-surface humidity conditions Td2m was analyzed instead of Rh2m as explained further in section 5. However, for the early years of the SMHIGridClim period the national Norwegian data set includes only a few Td2m observations but more Rh2m observations. Therefore, for Norwegian data all Td2m observations have been calculated as a function of observed T2m and Rh2m. The relationship used between Rh2m, T2m and Td2m is:

$$Rh2m = 100*\exp((17.625*Td2m) / (243.04+Td2m)) / \exp((17.625*T2m) / (243.04+T2m)),$$

with unit °C for T2m and Td2m. Finally all Td2m observations from all data streams have been checked so they do not exceed observed T2m. If any reported Td2m observation is higher than the corresponding T2m+5 the Td2m observation has been set to missing value. Any reported Td2m value in the range T2m to T2m+5 is set to its corresponding T2m value.

For daily maximum and minimum temperatures the 24h reported values valid at 18 UTC was used and for precipitation and snow depth the daily observations valid at 06 UTC are used. The observation availability for Tn and Tx with respect to 12h reporting intervals was examined but did not give any extra information.

2.3 BUFR observations

In addition to observations from national meteorological services, we extracted data from the MARS archive at ECMWF. Here, observational data are stored in BUFR-format. BUFR (Binary Universal Form for Representation of meteorological data) is a binary data format maintained by WMO. For our purpose, we extracted all available land surface data (LSD), see https://confluence.ecmwf.int/pages/viewpage.action?pageId=149339604. Moreover, the data is organized in different streams. Following the recommendation of ECMWF's experts (personal communication with Cornel Soci), we fetched data from different classes and streams in the same manner as it was done for the production of ERA5 (Hersbach et al., 2020). A bufr2ascii python script, utilizing ecCodes Version 2.18.0 python library, was used to extract the SYNOP station observations from the ECMWF BUFR files. The script follows this example on the ECMWF confluence pages: https://confluence.ecmwf.int/pages/viewpage.action?pageId=46600851. The BUFR SYNOP observation keys extracted are airTemperatureAt2M, dewpointTemperatureAt2M and totalSnowDepth.

2.4 ECA&D observations

The ECA&D observation data set (Klein et al., 2002) was considered for use in the SMHIGridClim analysis, however in the end we only used it for comparison and discussion of observation density with respect to other observation data sets. The reason for this is partly that the ECA&D time stamps of observations vary between countries and periods which made it too time consuming for integration in the analysis itself.

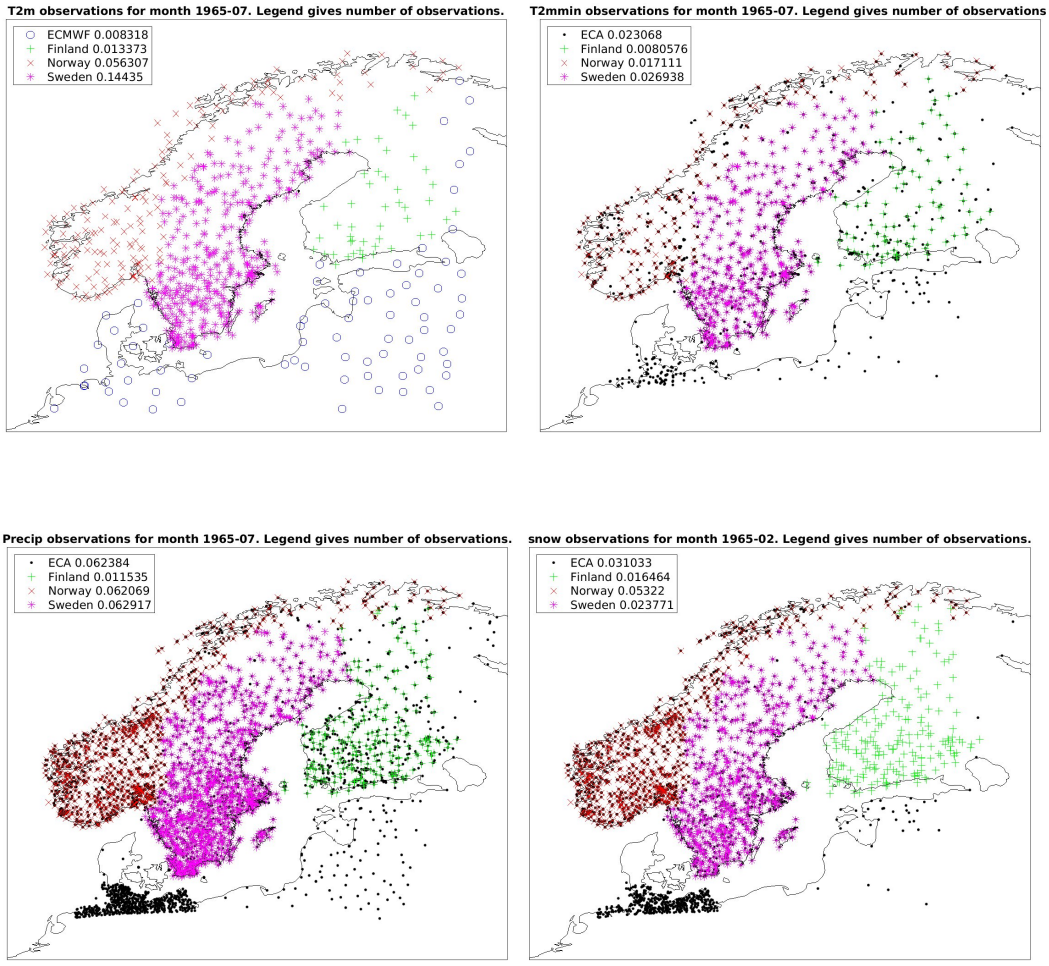

*Figure 2.2 Observation density maps of T2m (upper left July 1965), Tn (upper right July 1965), RR (lower left July 1965) and SD (lower right February 1965). The maps include observations from the different data sources BUFR (blue o), Norway (red x), Sweden (magenta *), Finland (green +) and ECA&D (black dots). The observations represent those that are available for the whole month taken into account that they are considered valid within specified limits. The numbers represent number of observations normalized by their corresponding representative areas, thus number of observations per month per km^2.*

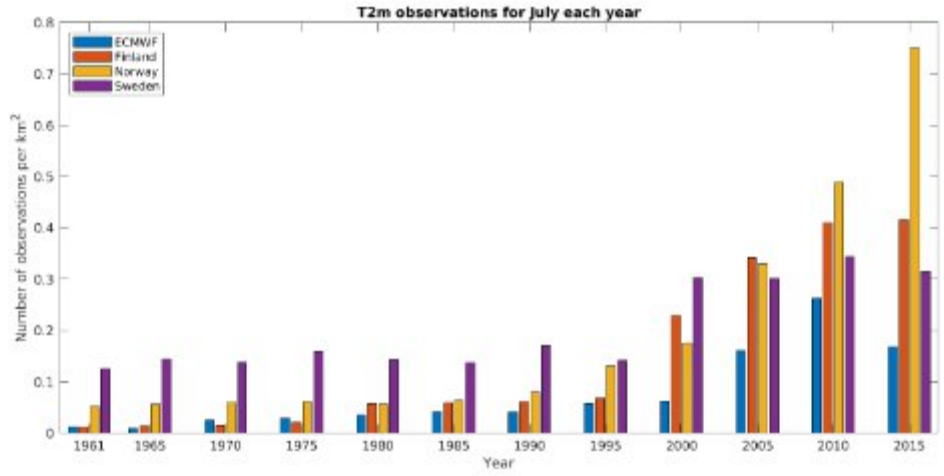
T2m observations for July each year
ECMWF
Finland
Norway
Sweden
Number of observations per km^2
0
0.1
0.2
0.3
0.4
0.5
0.6
0.7
0.8
1961
1965
1970
1975
1980
1985
1990
1995
2000
2005
2010
2015
Year

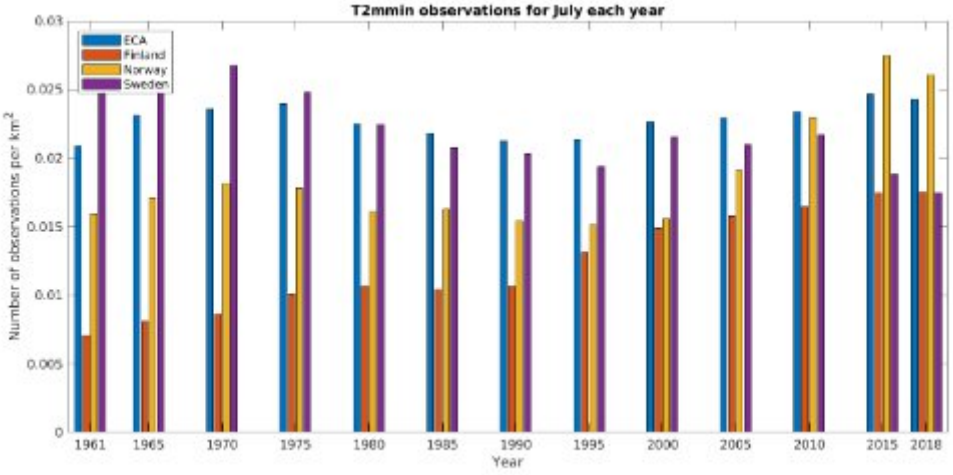
T2mmin observations for July each year
ECA
Finland
Norway
Sweden
Number of observations per km^2
0
0.005
0.01
0.015
0.02
0.025
0.03
1961
1965
1970
1975
1980
1985
1990
1995
2000
2005
2010
2015
2018
Year

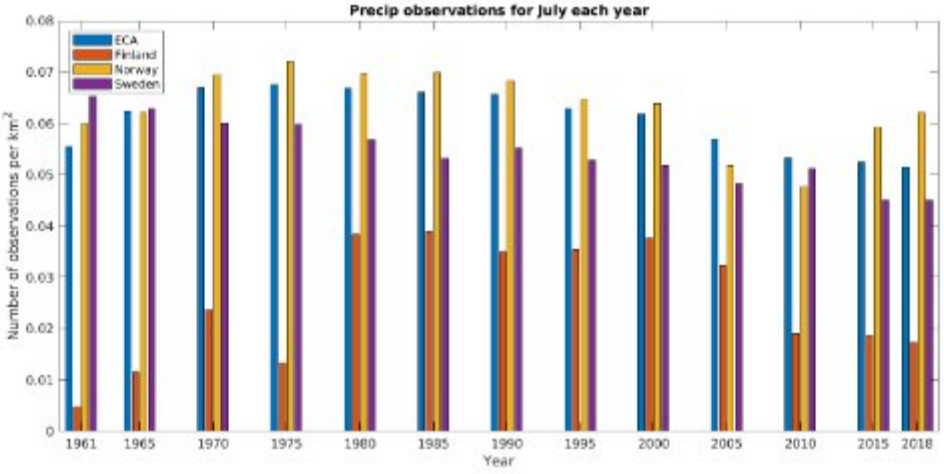
Precip observations for July each year
ECA
Finland
Norway
Sweden
Number of observations per km^2
0
0.01
0.02
0.03
0.04
0.05
0.06
0.07
0.08
1961
1965
1970
1975
1980
1985
1990
1995
2000
2005
2010
2015
2018
Year

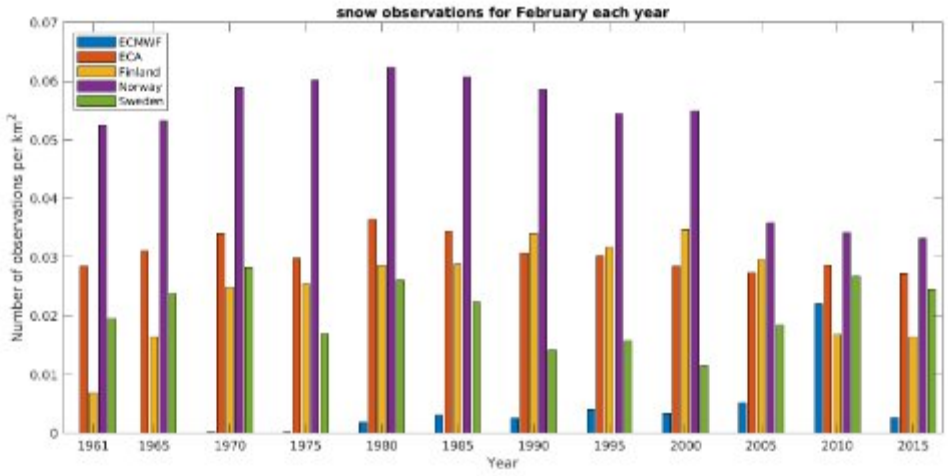

Figure 2.3 Observation density bar plots per year for (top to bottom) T2m (July), Tn (July), RR (July) and SD (February). The bars are colour coded with respect to data sources BUFR from ECMWF, Norway, Sweden, Finland and ECA&D. The observations represent those that are available for the whole month taken into account that they are considered valid within specified limits. The numbers represent number of observations normalized by their corresponding representative areas, thus no obs per month per km^2.

2.5 Observations density in space and in time

The spatial density of observations vary over time, considering both decadal time scale and diurnal time scale, and depends also on which observed quantity is considered. Figure 2.2 shows examples of the distribution of T2m, Tn (Tx is the same), RR and SD in 1965. In Appendix A similar plots for every 10 years are presented. The plots include positions of all valid observations for a specific month meaning observed values within reasonable limits and where metadata for position and altitude exists. For T2m and Sn it is clear how important the national data sets are since the available BUFR data are very limited during the early years of the SMHIGridClim period. For Tx, Tn and RR the national datasets are crucial since no BUFR data are available here. Although ECA&D observations are not used its coverage is good in Scandinavia. However, outside Scandinavia its coverage is very variable.

The observation density on decadal time scale is shown in Figure 2.3. The increase in T2m observations after 1995 is explained by the increase of automatic weather stations which partly increase the density but very much so the frequency in observations which means more stations with hourly reporting. The Tn figure reflects more the increase in network density since these observations are always reported only once per day. The RR observations show a decreasing trend in number from the 1980s and onwards for all data streams. The network of snow observations, also daily, does not show any clear trend for Sweden or Finland. However, the Norwegian network density shows a clear reduction between 2000 and 2005.

No figures are shown for how number of observations per hour over the day for T2m and Td2m vary on decadal time scale but an analysis of the numbers show that it is not meaningful to analyse more than every 6th hour for the period 1961-1967 and every 3rd hour for the period 1968-1996. From 1997 and onwards the automatic weather station network is dense enough to allow an analysis for every hour over the day although the density of observations still vary considerbale between the traditional reporting hours and the intermediate ones.

The northern part of Scandinavia shows some data sparse areas. Noticeable are an area in northern Finland, close to the Swedish border and an area in northern Sweden close to the Norwegian border. For such relatively data sparse areas the analysis will show larger uncertainty.

The data density seems to be comparable between the ECA&D data set and the national data sets for Tn, Tx and RR. However, there are station locations in the ECA&D data set not represented in the national data sets. The reasons for this are not understood and have not been further investigated in this project. ECA&D observations for snow depth over Finland seem to be missing for unknown reasons.

3 Observation quality control

For the observation quality control the TITAN package (https://github.com/metno/TITAN/wiki) developed at Met.Norway (Båserud et al., 2020) was used. Please note that this TITAN package is now being replaced by titanlib (https://github.com/metno/titanlib/wiki) and future applications will probably be better based on titanlib. However, at the time of this project titanlib was still not mature enough to be used for production.

The required input data for TITAN is station position (latitude and longitude), station altitude and the observation to be checked. All provided observations are assumed to be valid for a certain time, thus TITAN does not correlate observations over time. TITAN offers a number of different quality checks and options (Båserud et al., 2020). The ones applied in this study are described in the following section. The TITAN output includes a Data Quality Control (DQC) code indicating if the observation is considered correct (DQC=0) or suspicious (DQC>0).

3.1 Digital Elevation Map check

By providing a Digital Elevation Map (DEM) at a given map projection and resolution as NetCDF file TITAN can check if the altitude specified for each observation station agrees to the DEM within certain limits (option --dem, DQC=5). The DEM used in this case is based on GMTED2010 (Danielson and Gesch, 2011) which is provided as SURFEX input format (GMTED2010_075.EHdr) at 250 m resolution via the SURFEX web page http://www.umr-cnrm.fr/surfex/spip.php?article134. This global data set has been processed by a SURFEX setup to provide a DEM at 500 m resolution for TITAN covering the area of SMHIGridClim. The allowed deviation (--dz.dem) between the DEM and the provided station altitude is set to 300 m. The DEM check is applied to observations of T2m, Td2m, Tn and Tx. In complex terrain areas, like for example the Norwegian fjord landscape, the DEM check may not be relevant since 500 m DEM resolution is still too coarse. For such areas the DEM DQC flag has not been considered (see the gridpp section for more information).

3.2 Digital Elevation Map fill

The DEM can also be used to fill missing elevation data (option --dem.fill). This option is applied to the precipitation and snow depth observations to allow for more observations to be used from the Finland observation dataset during the period 1961-1979 when elevation data are missing for some stations. The DEM fill option has no impact if elevation is specified in the input data.

3.3 Missing observations or meta data

If any of the input data includes Not a Number the observation is flagged as missing data or metadata with DQC=1.

3.4 Plausibility range

If an observation is outside specified bounds (--vmin and --vmax) the observation is flagged as failing the plausibility test with DQC=2.

3.5 Buddy check

The buddy check (DQC=4) compares the observations against the average of all neighbours in a square box centred on each observation. The distance (--dr.buddy, default 3000 m) from the central observation to the sides of the box is specified. A minimum number of observations (--n.buddy, default 5) is required to be available in the box, and the range of elevations must not exceed a specified threshold (--dz.buddy, default 30 m). Several buddy checks in a row can be specified by the desired number of iterations (--i.buddy, default 1). The observation is flagged as suspicious if the deviation between the observed value and the box-average normalized by the box standard deviation exceeds a predefined threshold (--thr.buddy, default 3). A minimum allowed value for the standard deviation can be specified (--sdmin.buddy). The buddy check is always applied by default in TITAN but especially adjusted settings have here been used for precipitation and snow depth observations. In practice, the default setting of dr.buddy=3000 m means that the buddy check will not have an influence on other variables in the SMHIGridClim observation network.

3.6 Spatial consistency test

The spatial consistency test (SCT, DQC=5) acts as a more sophisticated buddy check by evaluating the likelihood of an observation given the values observed by the neighbouring stations (Lussana et al., 2010). The SCT is performed independently over several subdomains of the region defined by a predefined grid with a number of rows and columns (--grid.sct). The grid boxes can be smaller for a dense observation network. For the SMHIGridClim area we have normally used 3x3 grid boxes except for the observations every 3rd hour after 1996, when the observation network is considered a bit more dense, where we have used 5x5 grid boxes. Depending on the sign of the cross-validation (CV) residual in Eq 4 of Lussana et al. (2010) there are a few options for the threshold in Eq 4 in TITAN: the threshold (--thr.sct) is used for both positive and negative CV residuals or thresholds are specified separately for positive (--thrpos.sct) and negative (--thrneg.sct) CV residuals. Apart from these mentioned options the default TITAN values are used for other SCT options. The SCT test is used as the main quality test for T2m, Td2m, Tn and Tx. For precipitation and snow depth it is also used but the thresholds are given quite high values which means that only quite extreme deviations will be flagged.

3.7 Duplicates

Stations can be reported in more than one observation data stream, e.g. in BUFR and in the Swedish national data. To avoid such duplicates in the analysis we apply the no-duplicates option in TITAN (--no_duplicates) where stations are not allowed to be located closer than 0.01 deg apart (--dup.match_tol_x 0.01) and 100 m apart in altitude (--dup.match_tol_z 100). If duplicates are identified the last station in the list is used. In SMHIGridClim we give priority to national data streams with respect to the BUFR data stream. The duplicates are removed before any other processing of observations are done in TITAN. Thus, there is no DQC flag indicating duplicates.

3.8 First guess check

Besides the checks done with TITAN prior to the analysis, there is also a gross error check done against the first guess in the script that does the analysis. However, there is one exception, the observations of daily precipitation are not compared to the first guess. The reason for this is that the true precipitation field may be very patchy and we do not want to risk losing important information regarding local showers that were missed by the forecast model.

The check is done by interpolating the first guess to the observation points using a bi-linear interpolation. For temperature this interpolation also takes into account height differences between the model grid and the observation site (-0.0065 K/m and -0.0017 K/m for t2m and dt2m respectively). The difference is then compared to the standard deviation of all these differences. If the difference at any given point is larger than three times the standard deviation it is considered as a gross error and the observation is removed.

3.9 Comments

The TITAN isolated station check has been deactivated for SMHIGridClim by setting the option --doit.isol to 2.

4 Downscaling the first guess

During the time period January 2016 - July 2019, data from both UERRA and MEPS was available. Data from this period was used to establish a relation, based on a linear least squares regression, between a given point in the subarea of the MEPS grid constituting the SMHIGridClim region (at 2.5 km) and its surrounding 4 x 4 neighboring points in the UERRA grid, at 11 km horizontal resolution.

An example with the T2m from UERRA (interpolated to the 2.5 km grid) and the corresponding downscaled field is given in Figure 4.1. In the right panel of the same figure it is shown how one gridpoint (dark red) in the 2.5 km grid (pink) is associated with its surrounding 16 nearest neighbors (dark blue) from the 11 km UERRA grid (light blue).

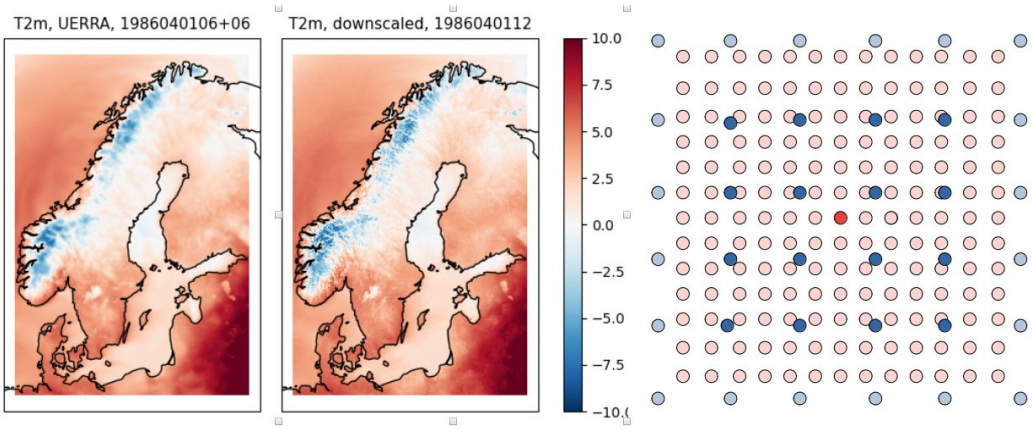

Figure 4.1 Example showing the downscaling of T2m. Left: Original UERRA field interpolated to the SMHIGridClim grid (unit: degrees Celsius). Middle: Downscaled field. Right: Schematic illustration of how a point (dark red) in the 2.5 km grid is associated with its 4x4 neighbourhood (dark blue dots) in the 11 km UERRA grid.

For T2m and Td2m, these linear least squares regressions were performed for nighttime (00 UTC) and daytime (12 UTC) as well as for the mid winter (represented by day number 0) and mid summer (represented by day number 183). The final weighting with respect to hour and time of the year was done combining the weights for day/night and winter/summer by using squared cosine functions centered around 00 and 12 UTC and at day number 0 and 183, see Figure 4.2. Thus resulting in 16 x 4 regression parameters for each point in the new grid for each of the parameters.

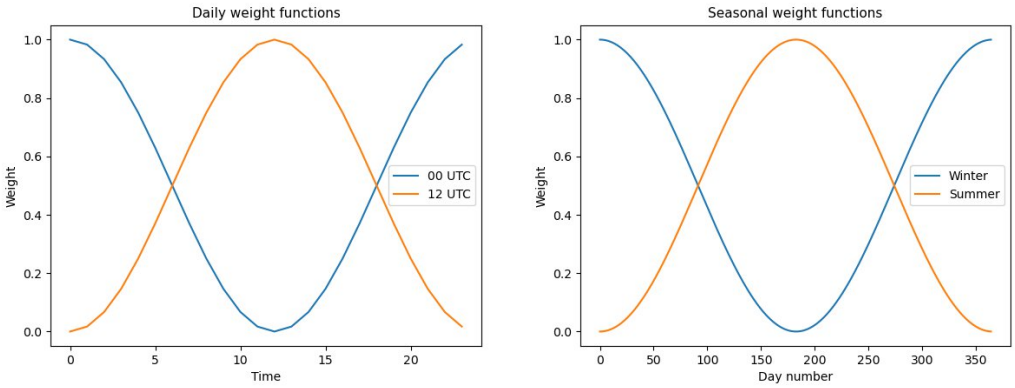

Figure 4.2 Weighting functions for the estimation and application of the downscaling parameters. Left: Daily weighting functions for 00 and 12 UTC parameters. Right: Weighting functions for the seasonal parameters at day number 0 (winter) and 183 (summer).

For Tn and Tx, no separate regression was done, instead the relations obtained for T2m were used for each of the twelve hours throughout the day (see Table 2.1). Weights for the downscaling of RR were obtained only based on seasonal weighing with no dependence of the hour of the day, and using a non-negative least squares solution to guarantee that the downscaled result should always be positive.

After the regression parameters have been estimated based on the overlapping time period for MEPS and UERRA, they are used in the downscaling of the UERRA grid for the entire data period. The same weighting functions that were used to find the regression parameters are again used to combine those parameters at any given date and time;

wd_00= cos((hr - 0) / 2 / 24*2*pi) ^2

wd_12= cos((hr - 12) / 2 / 24*2*pi) ^2

wy_w= cos((dn - 0) / 2 / 365.25*2*pi) ^2

wy_s= cos((dn - 365.25 / 2) / 2 / 365.25*2*pi) ^2

Here wd_00 and wd_12 are the weights associated with the given analysis hour (hr) while wy_w and wy_s are the seasonal weights associated with the analysis day number (dn). These weights are then used in a linear combination of the regression parameters associated with 00 UTC during winter and summer (w00w, w00s) and 12 UTC for the two seasons (w12w, w12a).

w= wd_00 * (w00w * wy_w + w00s * wy_s) + wd_12 * (w12w * wy_w + w12s * wy_s)

As described above, only a seasonal weighting was applied for the daily precipitation. For the downscaling of Tn and Tx, each of the fields associated with the 12 intervals in Table 2.1 were downscaled separately using the midpoint for each interval in the calculation of the weights. Constant weights were used for the downscaling of the daily

snow water equivalent.

Downscaling of the snow depth was done in three steps. First the snow water equivalent from UERRA was downscaled. Then it was divided by the snow density from UERRA, interpolated to the SMHIGridClim grid, to result in an estimate of the snow cover. A third step was then introduced to correct for large systematic differences between the probability distributions of the downscaled and observed snow depth data. The reason behind these differences has not been analyzed. The third step consisted of imposing an upper limit of 10 m to the downscaled snow depth followed by a quantile mapping (QM) of the downscaled values (Panofsky and Brier, 1968). The QM method has been shown to produce good results when it comes to correction of systematic erros, e.g. for removing precipitation biases (Themeßl et al., 2012).

5 Analysis with gridpp

The analyses were done using the open source software gridpp from the Norwegian Meteorological Institute (https://github.com/metno/gridpp). We used the python library version of gridpp that provides functions for doing an analysis using optimal interpolation (OI) to combine observations and gridded forecasts (the first guess) in a statistically optimal sense (Gandin, 1965). Besides optimal interpolation the library also provides functions for other operations like bi-linear interpolation and diagnosing entities, like was done here for relative humidity from the two meter temperature and two meter dew point temperature.

In order to perform an OI analysis one needs to provide information about the spatial covariances for the first guess error and the observation error. In gridpp the covariances are separated into an error variance ratio and a correlation (structure) function where the latter can be modeled in different ways.

We chose the more versatile function “BarnesStructure” (Barnes, 1973). Here the first argument is the horizontal decorrelation length scale (in meters) and the second is the vertical decorrelation length scale (in meters). A third argument specifies the decorrelation length across land area fraction (units 1), and a fourth argument specifies the maximum length that an observations will have an effect (in meters, also called the localization radius). In our case we set the last argument to zero implying that all observations will be considered.

In order to find suitable values for the parameters regarding the error variance, ratio between first guess and observations error variances as well as the parameters for the structure function we performed a cross validation. Such a procedure is also provided for by gridpp, that computes the analysis in a "leave-one-out" cross-validation fashion. For each output point, the observation at that point is left out of the OI analysis in order to provide an estimate of the error at that location. Note, however, that this error may not be representative for the scale at which the OI analysis is performed. Still, it provides valuable information regarding how well the analysis matches the observations in an independent way.

Using the cross validation functionality we set up an optimization scheme where we minimized the squared cross validation error using a grid search method. The minimization was done in a semi separable way. First the ratio between the observation and first guess errors and the horizontal correlation lengths were optimized together, assuming no vertical or land area fraction dependencies. Then the vertical correlation length was optimized on top of this result, and finally the land fraction correlation distance was optimized.

When the vertical and land area fraction correlation distances were optimized, only observation points whose neighbors differed with respect to these entities were

considered. Here the 75 percentile of the standard deviation of the differences in height and land area fraction was used as a threshold to determine which points should enter the minimization. This was done in order to highlight the cases where differences in these entities matter.

Since the optimal parameters of the structure function depends on the observation density we derived a set of optimal parameters throughout the time period 1961 - 2018. Optimal parameters were derived for the years 1965 (extended to 1961), 1975, 1985, 1995, 2005, and 2015 (extended to 2018). Again, separate parameters were assigned to night and day as well as winter and summer using the same weighting functions as for the downscaling, with an extra 10 year wide weighting around the specific year:

(cos((yr-yr_k) / 2 / 20*2*pi) ^2)

Parameters for any given year and date throughout the time period 1961 - 2018 were then obtained by a smooth spline interpolation.

The analyses were done using the downscaled fields, described earlier as the first guess, with one exception. The analysis of the relative humidity was not done directly with gridpp. Instead it was diagnosed with the gridpp function gridpp.relative_humidity using the analyzed T2m and Td2m fields as input. The reason for this is that the errors of the T2m and Td2m first guess fields better fits a normal distribution than that of the Rh2m field which is bounded to the range 0 - 100 % and hence also has an error that is bounded close to its extremes.

6 Results

In the following sections, results of the data processing steps are presented. In section 6.1 the downscaling of UERRA forecasts is evaluated in terms of the average difference between the downscaled fields for the first guess, and the original UERRA fields. Section 6.2 presents the result of the optimization of parameters for the gridpp analysis. In 6.3 climatologies of the output data from the analysis are presented, and in 6.4 the influence of the analysis are described in terms of the analysis increments, which are the difference between the analysis and the first guess. Section 6.5 gives an overview of the spatial patterns of analysis errors calculated with gridpp. Finally, in section 6.6 time series of yearly cross validation statistics for the analysis are presented..

6.1 Downscaling

This section describes how the downscaled fields for T2m, Td2m, Tn, Tx, RR and Sn compare to the original UERRA forecast fields on a daily and seasonal basis. In order to make the comparison on the same grid, the UERRA fields were interpolated to the SMHIGridClim grid using bi-linear interpolation.

The downscaling procedure results in fields that fit the patterns in the corresponding MEPS fields during the years 2016 - 2018. The assumption is that the performance of the MEPS forecast is superior to that of the UERRA forecast. How the downscaling affects the analysis performance is described in the section 6.7 regarding the cross validation results.

6.1.1 Two meter temperature

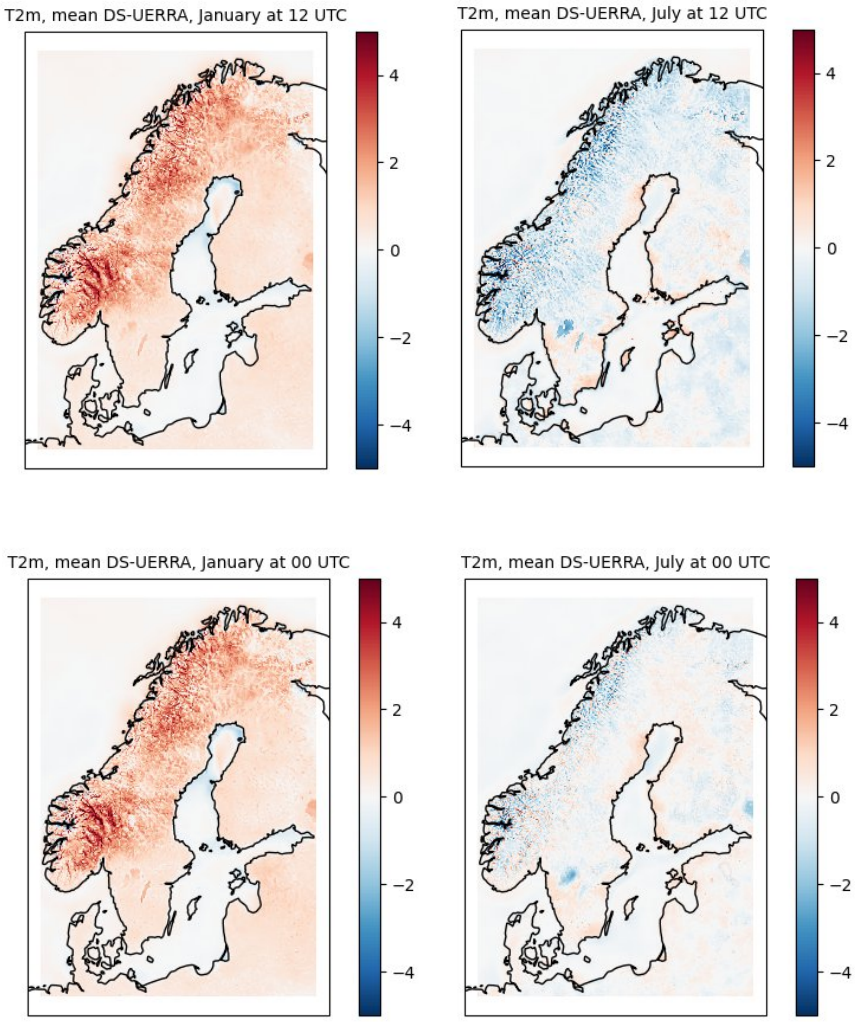

Figure 6.1 Mean differences between T2m from the downscaled and original UERRA fields respectively (unit: K). Top left: January 12 UTC. Top right: July 12 UTC. Bottom left: January 00 UTC. Bottom right: July 12 UTC.

In the winter (represented by January) the downscaling results in higher temperatures, both during night and day (figure 6.1). In the summer (July) it is the other way around, with the downscaling mostly producing colder temperatures, especially in the mountains during the day. Note that lakes Vänern and Vättern get slightly warmer during winter and noticeably colder during summer.

6.1.2 Two meter dew point temperature

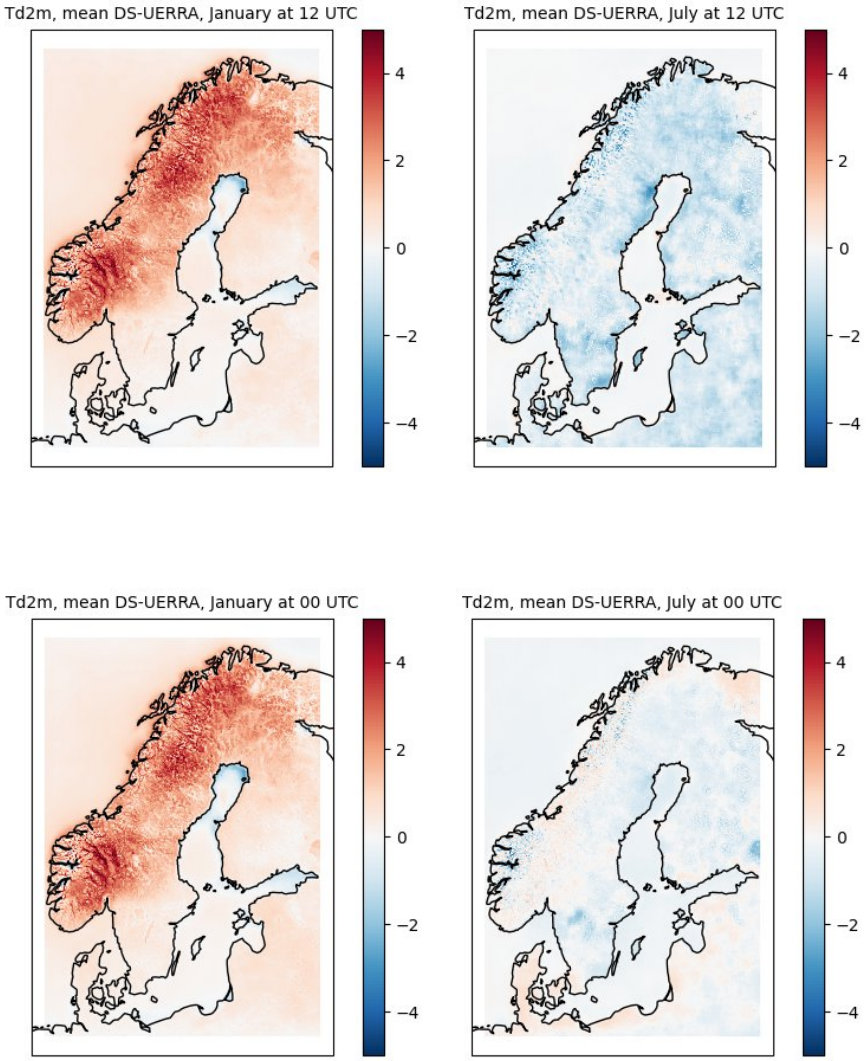

Figure 6.2 Mean differences between Td2m from the downscaled and original UERRA fields respectively (unit: K). Top left: January 12 UTC. Top right: July 12 UTC. Bottom left: January 00 UTC. Bottom right: July 12 UTC.

Figure 6.2 illustrates the mean differences between the downscaled Td2m fields and the original UERRA fields for night and day (00 and 12 UTC) as well as winter (January) and summer (July).

The pattern for the dew point temperature is similar to that of T2m. However, the temperature increase during the winter is more pronounced. The cooling during the summer day is more homogenous throughout the area while the effect is rather neutral for the summer night. The downscaling effect on the dew point temperatures of lakes Vänern and Vättern is reduced compared to that of T2m.

6.1.3 Daily minimum and maximum temperature

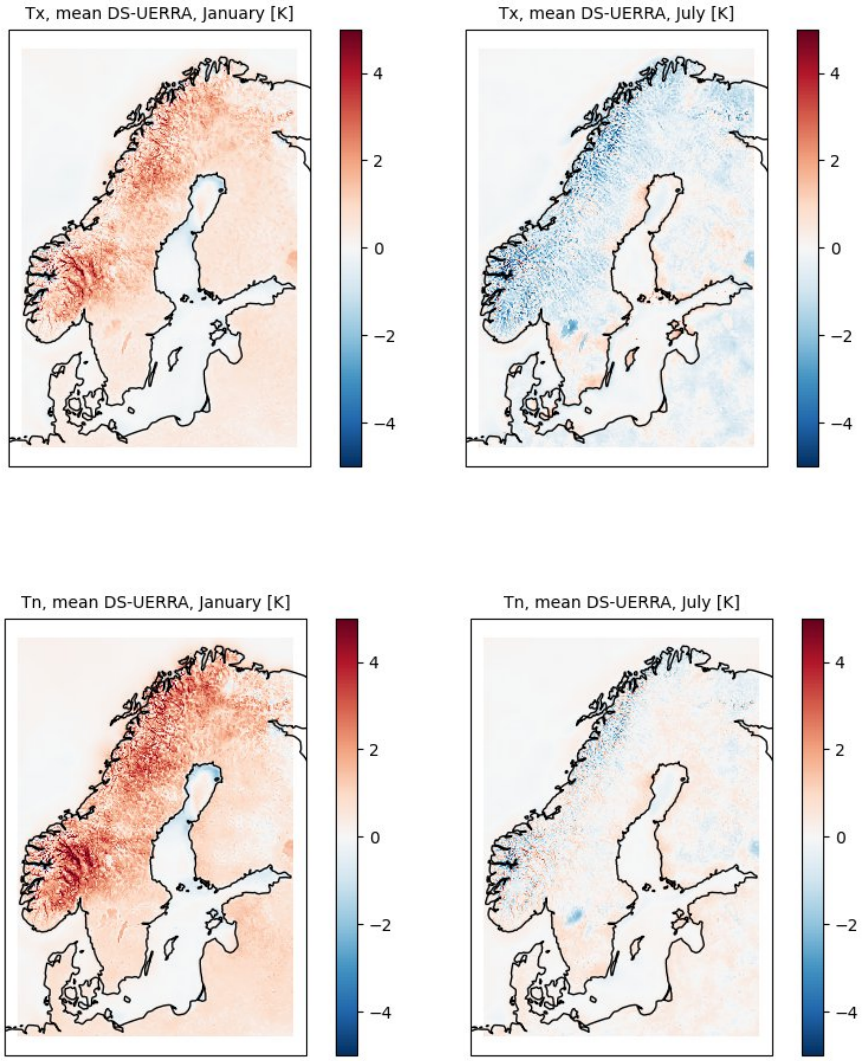

Figure 6.3 Mean differences between Tn and Tx from the downscaled and original UERRA fields respectively (unit: K). Top left: Tx, January. Top right: Tx, July. Bottom left: Tn, January. Bottom right: Tn, July.

Figure 6.3 shows the mean differences between the downscaled Tn and Tx fields and their original UERRA counterparts during winter (January) and summer (July).

It comes as no surprise that the patterns for Tn and Tx are very similar to those of the two meter temperature at 00 and 12 UTC.

6.1.4 Daily precipitation

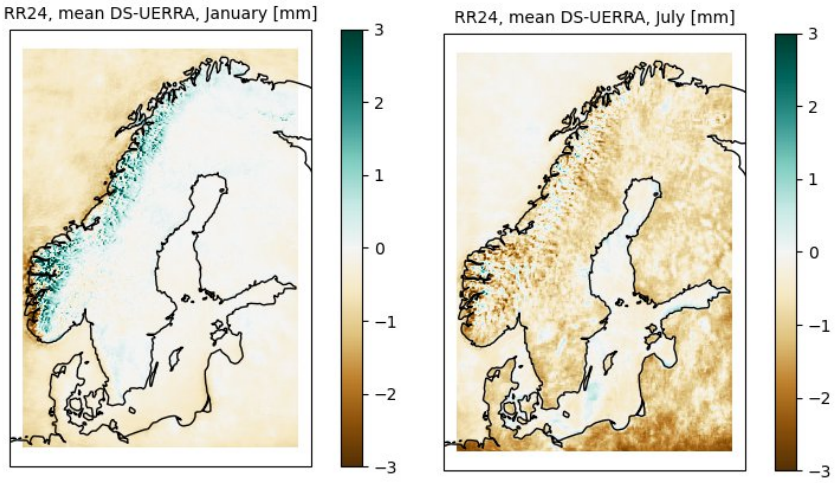

Figure 6.4 Mean differences between downscaled RR24 and the original UERRA fields. Left: January. Right: July.

Figure 6.4 shows the mean differences in daily precipitation between the donwscaled fields and their original UERRA counterparts during winter (left) and summer (right). During winter the downscaling intensifies the precipitation in the mountains. For the summer period, the downscaling instead results in a general decrease in the daily precipitation

6.1.5 Daily snow depth

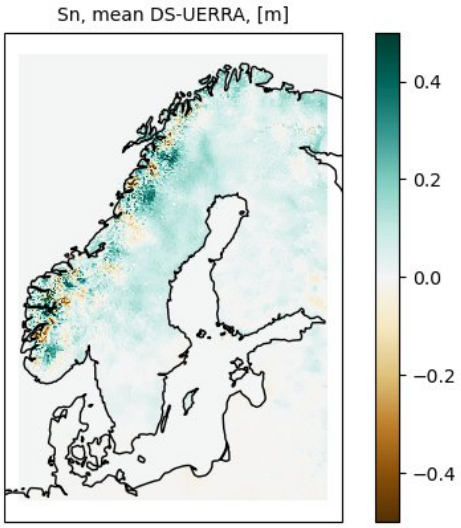

Figure 6.5 Mean differences between downscaled Sn and the original UERRA fields. The color scale was limited to +/- 0.5 m to reveal more details.

Figure 6.5 shows the mean differences in daily snow depth between the donwscaled fields (including the quantile mapping) and the UERRA estimate based on the ratio between snow water equivalent and snow density. The largest differences can be seen in Norway

and in the mountain areas. There is a slight trend towards more snow in the downscaled fields at higher latitudes.

6.2 Gridpp parameters

The gridpp parameters regarding error ratios and correlation distances were optimized using weighting functions centered around six reference years; 1965, 1975, 1985, 1995, 2005 and 2015. Smooth spline functions were then used to interpolate the optimal parameters to any given year during the time period 1961 - 2018.

6.2.1 Two meter temperature

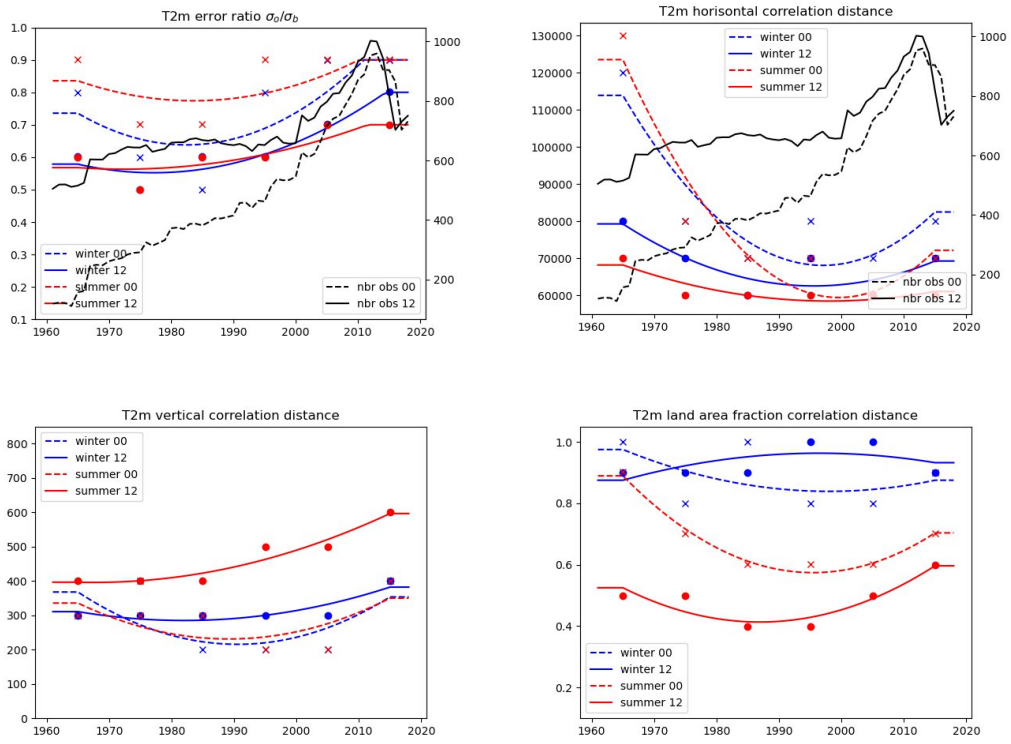

Figure 6.6 Time interpolation of optimized gridpp parameters. Black lines show the mean number of observations per analysis date on the axis to the right. Top left: Error variance ratio (unitless). Top right: Horizontal correlation (unit: m). Bottom left: Vertical correlation (unit: m). Bottom right: Land area fraction correlation (unitless).

The optimal gridpp parameters for the two meter temperature, and how they are interpolated in time, is illustrated in Figure 6.6. Also shown (in the top panels) is the evolution of the mean number of observations available for the T2m analysis at 00 and 12 UTC respectively. The optimal parameter values for the six reference years are shown with crosses and dots for night (00 UTC) and day (12 UTC), while the corresponding interpolated values are shown with dashed and sold lines respectively.

The ratio between the error variance of the observations and the error variance of the first guess (top left panel of Figure 6.6) shows a small increase with time. This probably corresponds to improved accuracy in the first guess (e.g. more observations used in the UERRA analysis from which the forecasts starts). The ratio is lowest during daytime when there is also little difference between winter and summer. It is then somewhat

higher during the summer night and highest during the winter night. The reasons for these differences have not been investigated.

The horizontal correlation distance is optimized together with the error ratio and shows a similar pattern (top right panel of Figure 6.6). Here the connection to the observation density is important and it is clear that the optimal analysis at the beginning of the time period needs larger error correlation distances than at the end. With a sparser observation distribution the structure functions (error covariance functions) need to be wider in order to get support from enough observations. Note that the number of observations during night time is much lower than during day time at the beginning of the time period and that this is reflected in wider horizontal correlation functions during the night.

The bottom left panel of Figure 6.6 shows the distance parameter for the vertical correlation function. Here there is little variation with the distance being somewhat longer at 12 UTC during summer.

Finally, the distance parameter with respect to differences in land area fraction is shown in the bottom right panel of Figure 6.6. The value is a bit higher during winter indicating that differences in land area fraction matter less during that season. This cloud be explained by the fact that water bodies can freeze during winter and then have temperatures more similar to their surroundings than what is the case during the summer season.

6.2.2 Two meter dew point temperature

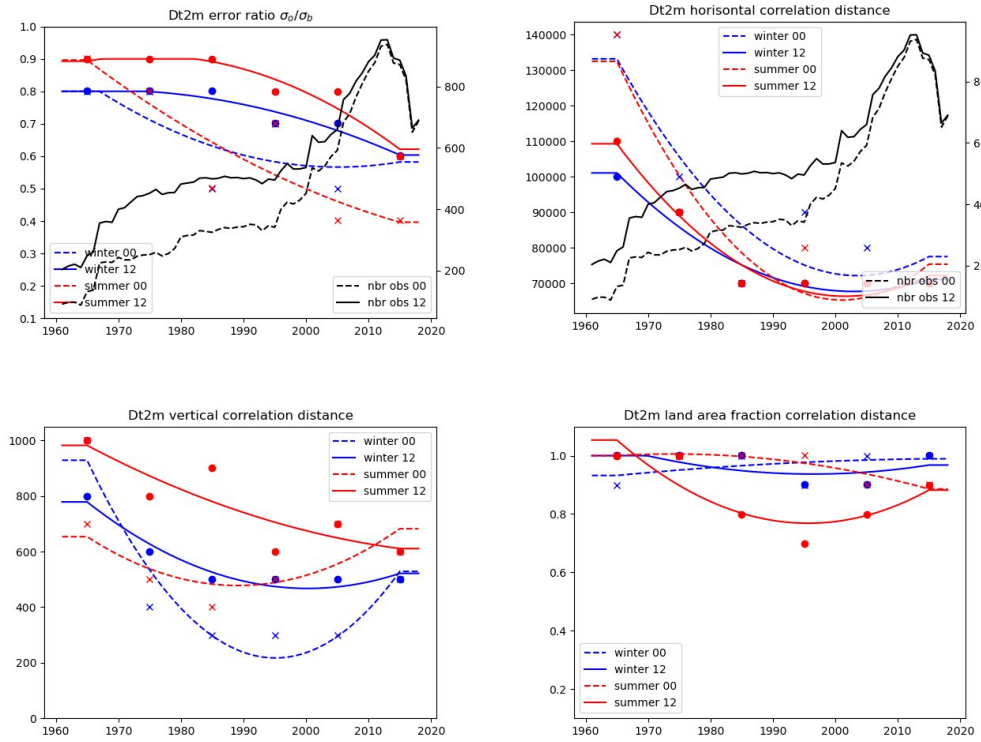

Figure 6.7 Time interpolation of optimized gridpp parameters. Top left: Error variance ratio (unitless). Top right: Horizontal correlation (unit: m). Bottom left: Vertical correlation (unit: m). Bottom right: Land area fraction correlation (unitless).

Optimal gridpp parameters for the two meter dew point temperature is shown in Figure 6.7. The legend is the same as for the two meter temperature described in the previous section.

For the dew point temperature, the error ratio decreases with time. This indicates that either the measurements have less noise or the first guess has larger errors towards the end of the time period. Why and if this is really the case has not been studied.

The horizontal correlation distance for the dew point shows a similar pattern to that of the two meter temperature where the increase in observation density is the natural explanation.

The vertical correlation distance shows a somewhat disparate pattern. However, the actual influence of these variations on the analysis performance is rather low.

Differences in land area fraction are less important for the dew point analysis. There is a tendency towards such differences being more relevant during summer noon compared to other times of the year. Again these parameter differences only results in minor effects on the analysis performance.

6.2.3 Daily precipitation

The optimization of the gridpp parameters for the daily precipitation resulted in very similar values for all the reference years. Moreover there was no significant difference between summer and winter.

Hence, the gridpp parameters for the daily precipitation were set to constant values for all analysis dates. The optimal values are given in Table 6.1.

Error variance ratio	Horizontal distance	Vertical distance	Land area fraction
0.30	43 km	1800 m	0.0

Table 6.1 Optimal gridpp parameters for the analysis of daily precipitation.

Note that a value of 0.0 for the land area fraction difference means that such differences have no effect.

6.2.4 Daily snow depth

The optimization of the gridpp parameters for the daily snow depth also resulted in very similar values for all the reference years. Since snow mainly occurs during the winter time no distinction was made between different seasons for this parameter.

The gridpp parameters for the daily snow depth were set to constant values for all analysis dates. The optimal values are given in Table 6.2.

Error variance ratio	Horizontal distance	Vertical distance	Land area fraction
0.90	35 km	350 m	0.55

Table 6.2 Optimal gridpp parameters for the analysis of daily snow depth.

6.3 Climatologies

Climatologies for the analyzed entities during the time period 1991-2018 (close to the climate standard normal period 1991-2020) are depicted in Figure 6.8. Note that the ranges for the relative humidity, yearly precipitation and daily snow depth have been clamped at the 1 and 99 percentiles in order to enhance the dynamic range. The temperatures where clamped at +/- 11 K for the same purpose.

In Figure 6.9 the differences between the climatological values of the same entities for the time periods 1991-2018 and the climate normal period 1961-1990 are shown.

For all the temperature related parameters a general increase is seen throughout the analyzed area. The largest increase is seen for the daily minimum temperature. Also the mean yearly precipitation is increasing with a maximum in the south-east part of Norway where the yearly precipitation is already at its highest. In Sweden the precipitation shows a noticeable increase in the west coast region. For the relative humidity the pattern is more patchy, but indicate increased values mainly in the northern part and somewhat decreasing values in the southern part of Sweden.

Note that there are some points standing out in the difference maps, mainly in coastal regions, and especially for the relative humidity and the precipitation. Most of these deviations are connected to coastal stations that are not representative on the scale of the grid used for the analysis. However, over Sweden, which is the focus area of this analysis, the fields looks rather smooth. The snow depth is in general decreasing over Sweden.

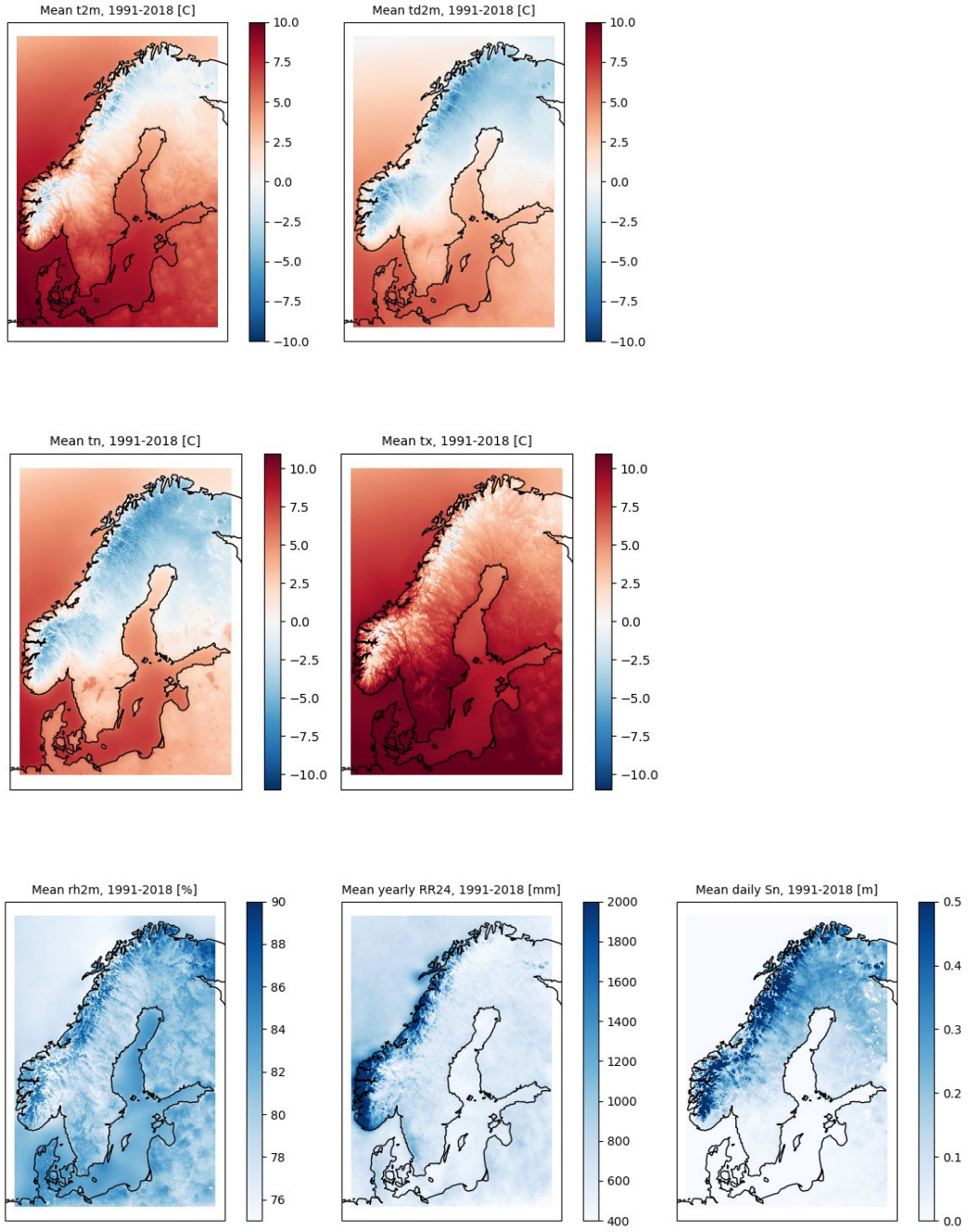

Figure 6.8 Climatologies based on the gridpp analyses for the time period 1991-2018. Top left: hourly mean T2m. Top right: Hourly mean Td2m. Middle left: Daily mean Tn. Middle right: Daily mean Tx. Bottom left: Hourly mean rh2m. Bottom middle: Yearly mean RR. Bottom right: Daily mean Sn.

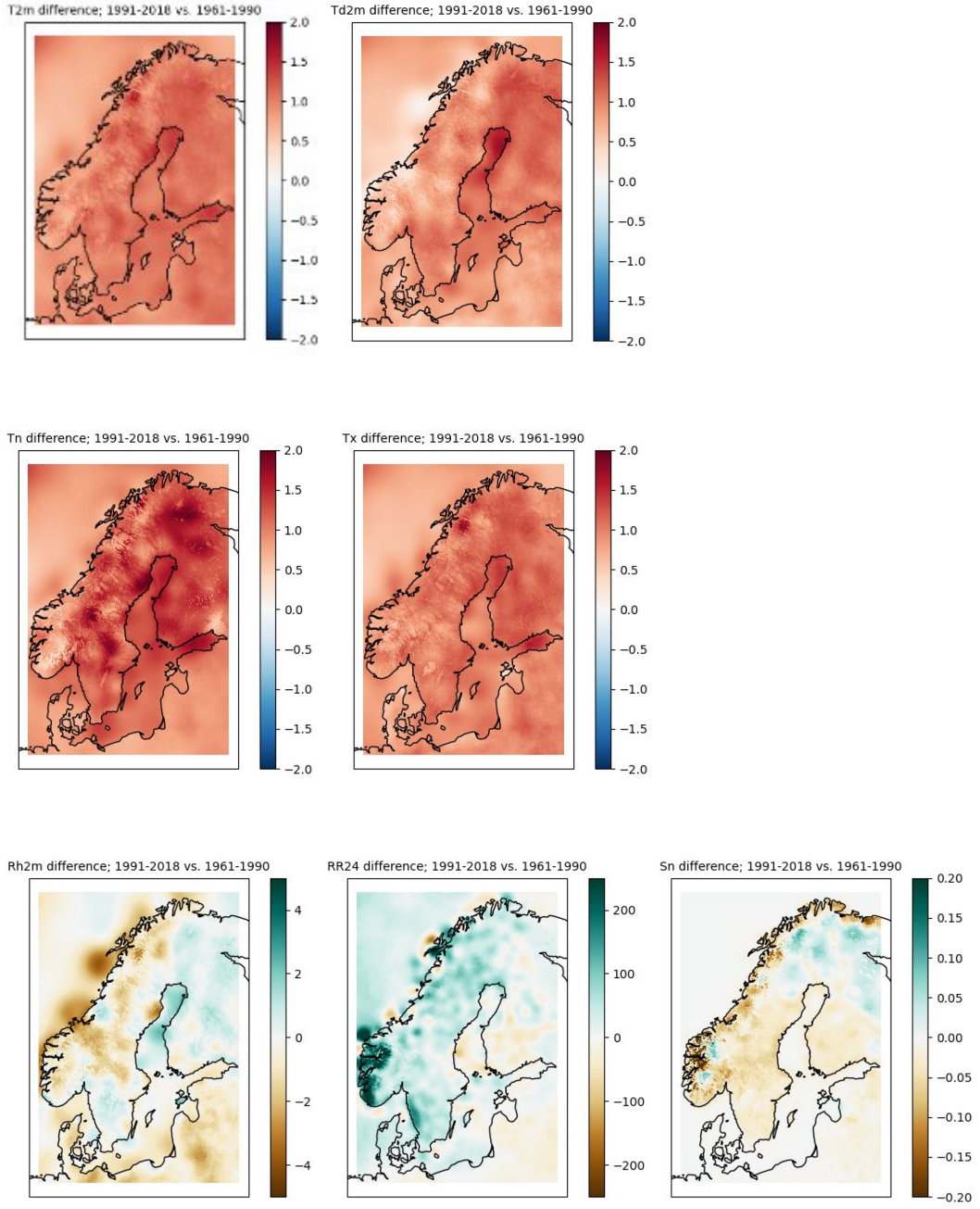

Figure 6.9 Differences between climatologies for the time periods 1991-2018 and 1961-1990. Top left: hourly mean T2m. Top right: Hourly mean Td2m. Middle left: Daily mean Tn. Middle right: Daily mean Tx. Bottom left: Hourly mean rh2m. Bottom middle: Yearly mean RR. Bottom right: Daily mean Sn.

6.4 Analysis increments

In this section the mean of analysis increments, which are the difference between the analysis and the first guess, is described. Note that this means that positive values in the maps indicate that the first guess was too low and the other way round. Ideally the distribution of the analysis increments should follow a normal distribution with zero mean. Here the first guess is given by the downscaled UERRA fields described earlier, with one exception. The first guess for the analysis of the relative humidity is instead diagnosed from the analyzed T2m and Td2m fields.

As part of the data quality control, analysis increments for every month during the data period was inspected manually.

6.4.1 Two meter temperature

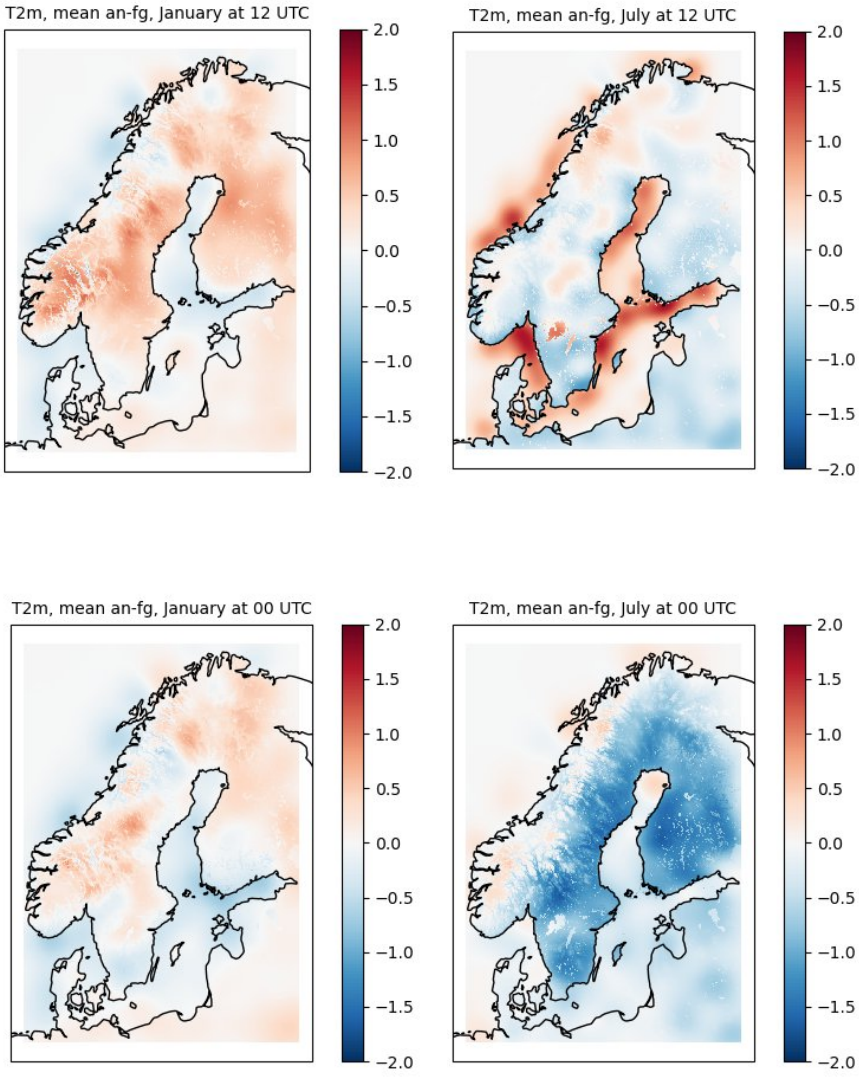

Figure 6.10 Mean analysis increments for T2m [℃]. Top left: January 12 UTC. Top right: July 12 UTC. Bottom left: January 00 UTC. Bottom right: July 00 UTC.

The analysis increments for the two meter temperature are illustrated in Figure 6.10. During the winter noon the analysis results in a systematic increase of the temperature

(top left panel) while it is the other way round during the summer night (bottom right panel).

This can be compared to the differences between the downscaled and original UERRA fields shown in Figure 6.1. The downscaling resulted in warmer fields during the winter days but not warm enough to fit the observations. For the summer night the downscaling was rather neutral indicating that both MEPS and UERRA have a positive bias for that period.

Note that the temperature of Lake Vänern was decreased by the downscaling during the summer but this effect is nullified by the analysis during the summer day.

6.4.2 Two meter dewpoint temperature

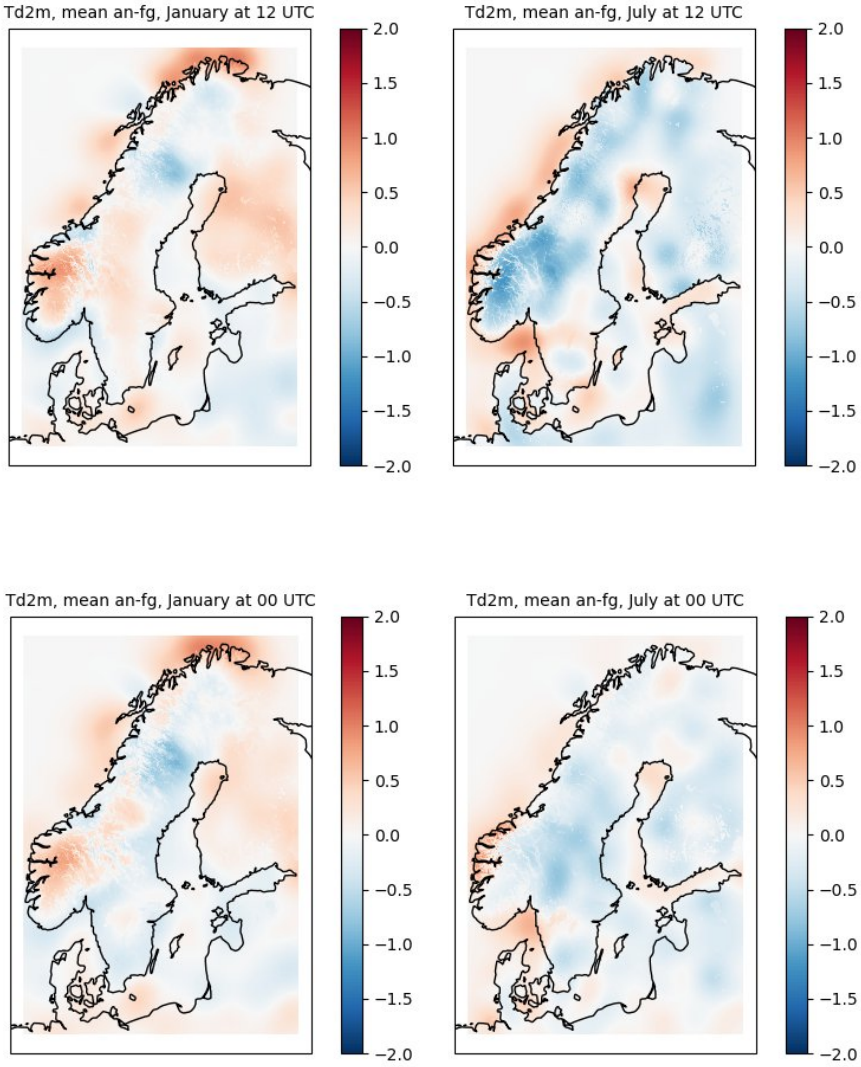

Figure 6.11 Mean analysis increments for Td2m [℃]. Top left: January 12 UTC. Top right: July 12 UTC. Bottom left: January 00 UTC. Bottom right: July 00 UTC.

Figure 6.11 shows the mean analysis increments for the two meter dew point temperature. The results look good during winter with no consistent bias patterns. During summer the analysis decreases the temperatures somewhat, both during day and night.

Comparing these results with those earlier presented for the down scaling of Td2m it can be seen that the temperature increase imposed by the downscaling during winter had a positive effect. The decrease during the winter daytime period was also in the right direction but not strong enough. The night time values during the summer are a bit on the high side as indicated in the lower right panel of Figure 6.11.

6.4.3 Two meter relative humidity

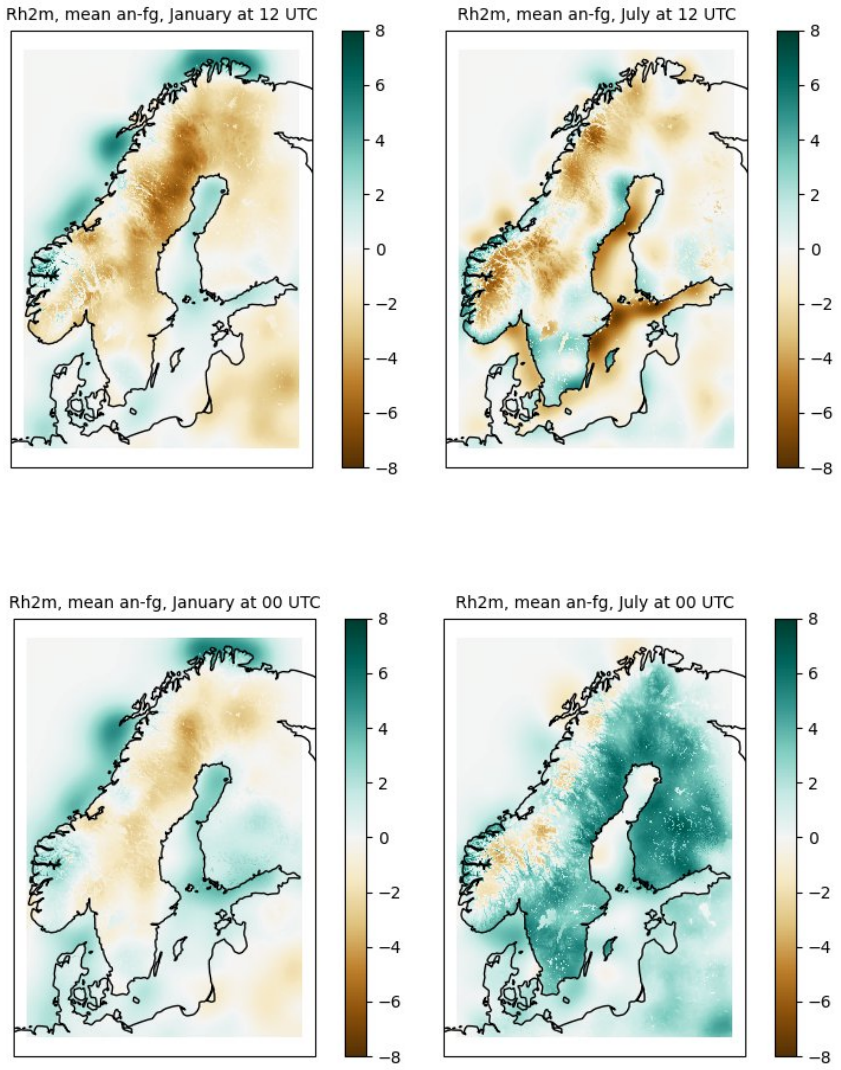

Figure 6.12 Mean analysis increments for Rh2m [% units]. Top left: January 12 UTC. Top right: July 12 UTC. Bottom left: January 00 UTC. Bottom right: July 00 UTC.

The analysis increments for the two meter relative humidity depicted in Figure 6.12 are not really analysis increments. Relative humidity is not analyzed per se, but instead diagnosed from the analyses of T2m and Td2m. Anyway it can be interesting to look at

the difference between Rh2m diagnosed from the downscaled fields of T2m and Td2m, and the diagnosed analysis. The results from such a comparison is shown in Figure 6.12.

The pattern follows that of T2m and Td2m. Since the analyses of T2m and Td2m showed a deficiency in the model input (first guess) during the warm summer and cold winter seasons, this is here reflected in too humid winter days (top left panel) and too dry summer nights (lower right panel).

6.4.4 Daily minimum and maximum temperatures

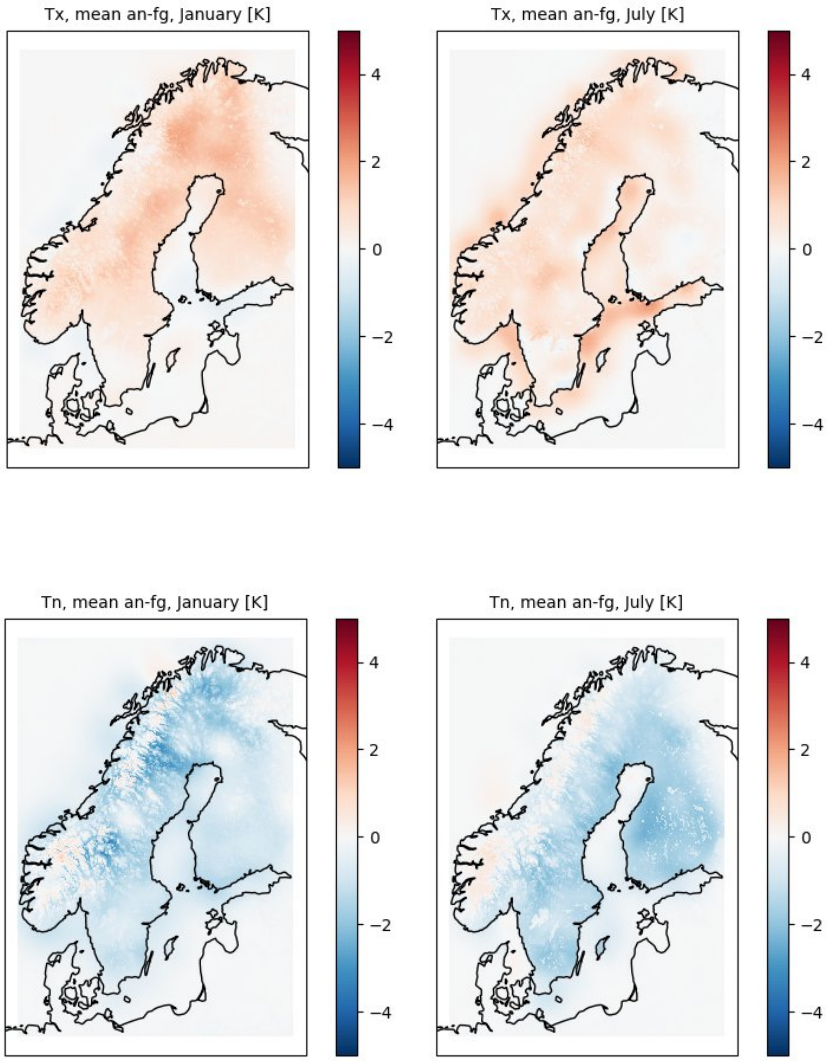

Figure 6.13 Mean analysis increments for Tn and Tx [℃]. Top left: Tx, January. Top right: Tx, July.. Bottom left: Tn January. Bottom right: Tn July.

It is well known that numerical weather prediction models have problems reproducing the extremes of the daily temperature cycle. This is also evident in Figure 6.13 where the mean analysis increments of the daily minimum (bottom panels) and maximum temperatures (top panels) are shown. The analysis changes the maximum to be warmer and the minimum to be colder than what is suggested by the first guess.

When this result is compared to how the downscaling affects the original UERRA forecasts, something peculiar emerges. The downscaling increases the minimum

temperature during the winter nights and decreases the maximum temperatures during the summer day time, contrary to what the analysis suggests.

The reason for this seems to be that the MEPS model is even worse at reproducing the daily cycle of the minimum and maximum temperatures than UERRA and that the downscaling then replicates this bad behavior.

6.4.5 Daily precipitation

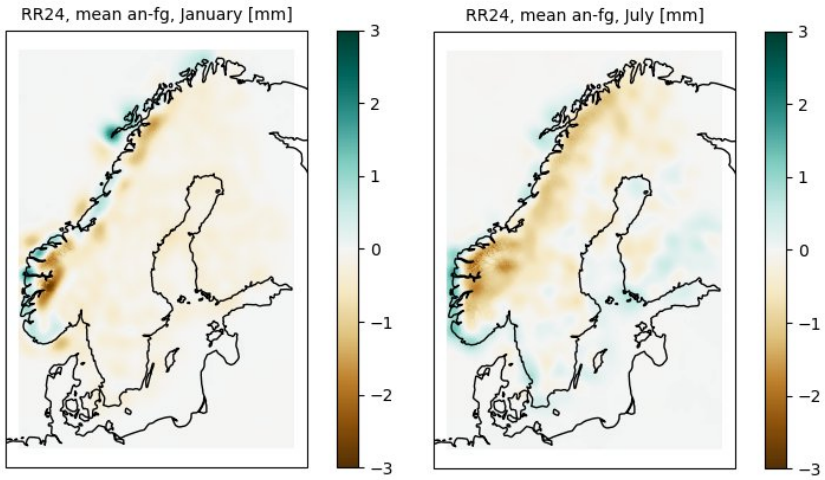

Figure 6.14 Mean analysis increments for the daily precipitation. Left: January. Right: July.

The analysis increments for the daily precipitation indicate that the first guess has too much precipitation in general and that the effect is largest in the Norwegian mountain regions, see Figure 6.14.

During summer, the first guess has too little precipitation along the south-west Norwegian coast and there is also a slight tendency that the first guess underestimates the precipitation along the Swedish west coast during the summer season (right panel).

Looking back at the results from the downscaling it is evident that the decrease of the precipitation in UERRA during summer was beneficial. The way the downscaling increases precipitation in parts of the Norwegian mountain chain is more questionable. However, this has not been reviewed in detail.

6.4.6 Daily snow depth

The analysis increments for the daily snow depth indicate that the first guess has too little snow in parts of the Norwegian mountain regions and in Finland, see Figure 6.15. The neutral result in the eastern part of Finland is due to a lack of observations in that region.

Comparing the analysis increments with the effect of the downscaling (Figure 6.5) it seems as if the downscaling was working in the right direction. However, there is one area north west of Östersund where the downscaling decreased the snow depth and the analysis then revered it by adding more snow.

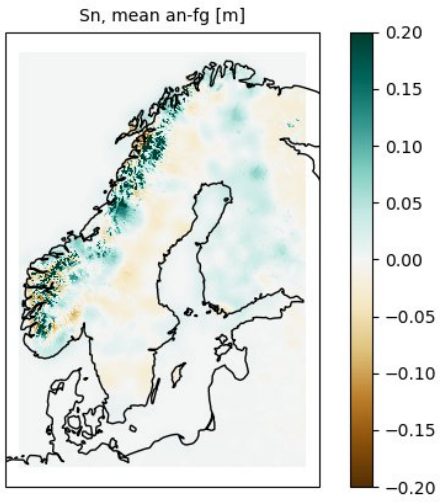

Figure 6.15 Mean analysis increments for the daily snow depth.

6.5 Analysis errors

The gridpp software can output an estimate of the analysis error, i.e. a map with the point-wise error variance in the output from the gridpp OI analysis. Here the error refers to the difference between the analysis and an imagined true value at any given point. The quality of this estimate depends heavily on the information the user provides regarding the observation and first guess error variances.

For the analysis, the user only has to specify the ratio between the observation and first guess error variances. However, in order to get an estimate of the analysis error these errors need to be specified separately.

The first guess error variance was estimated as the variance of the error between the first guess and the observations at any specific analysis date. This means that it is set to a constant field but that this constant varies over time, depending on how well the first guess fits the observations.

The observation error was then calculated by multiplying the estimated first guess error variance with the gridpp error ratio parameter obtained from the optimization. Hence, also the observation error variance field will be constant in space but vary over time.

The spatial variation in the analysis error comes from the way the structure function, depending on horizontal, vertical and land area fraction distances, interacts with the current observational network.

In the light of the above assumptions the absolute values of the analysis errors should only be viewed as crude estimates. However, the spatial patterns carries important information about how the analysis error varies with respect to the underlying observation network.

Analysis errors for every month during the data period was inspected manually as part of the data quality control.

.

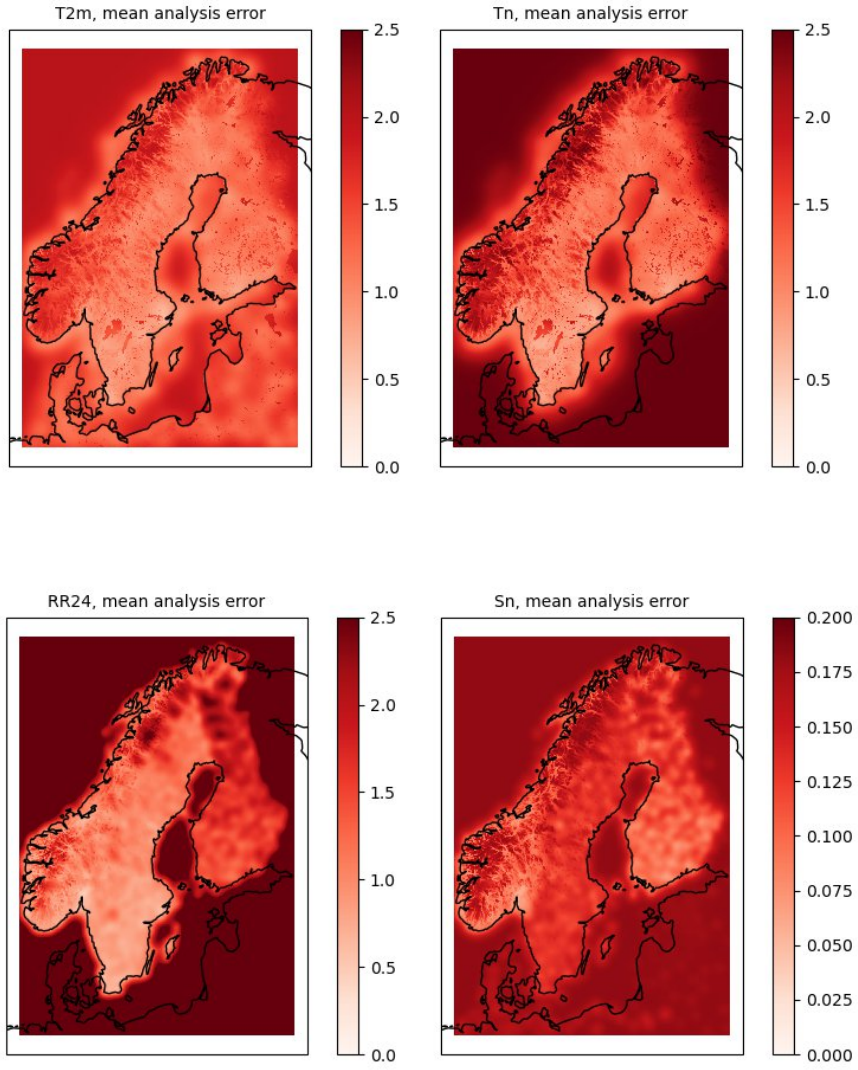

Figure 6.16 Mean analysis errors. Top left: T2m (unit: K). Top right: Tn (unit: K). Bottom left: RR (unit: mm). Bottom right: Sn (unit: m).

Figure 6.16 illustrates the mean analysis errors (at 00, 06, 12 and 18 UTC) for T2m, Tn, RR and Sn over the entire time period 1961 - 2018. The error for Td2m is very similar to that of T2m and that of Tn and Tx, albeit with somewhat lower values.

Note the difference in the error between areas where there are observations and areas where only the first guess is present. For the analysis of T2m and Td2m also observations from the ECMWF MARS archive entered the process. This results in an analysis error that is rather homogenous within the SMHIGridClim area (upper left panel of Figure 6.16). Some differences can be noted. The variable orography in Norway seems to pose a challenge for the NWP forecasts causing the error to be larger there than in the flatter areas of Sweden and Finland. The area east and south of Finland show a larger error that is probably due to fewer observations in these regions.

For Tn/Tx, RR and Sn only observations from Norway, Sweden and Finland entered the analysis. This is reflected in the analysis error being much larger outside this area. The relative difference between the error in areas with and without observations is most pronounced for the daily precipitation (bottom left panel of Figure 6.16). The legend was

clamped for both Tn, RR and Sn in order to make details visible in the region where observations contribute to the analysis.

6.6 Cross validation

In order to obtain a better estimate of the analysis error the cross validation results was examined. As mentioned earlier, the gridpp software can perform an efficient "leave-one-out" cross validation and this was used in order to find what parameters to use in the optimal interpolation with gridpp.

However, in the production of the SMHIGridClim analysis a cross validation was also done at each analysis date. Hence there are cross validation estimates of the analysis error available at each observation point for any given analysis (except for Rh2m that was diagnosed).

In the following sections the performance of the original UERRA data, the corresponding downscaled data and the resulting analysis are compared with respect to bias, standard deviation and root mean squared error.

6.6.1 Two meter temperature

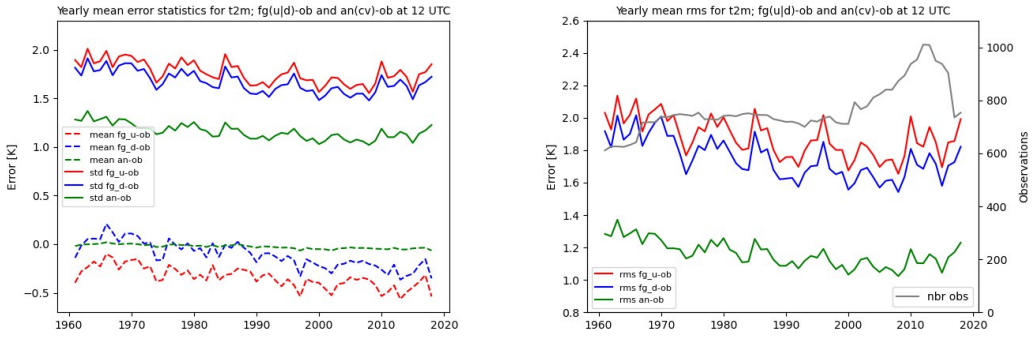

Figure 6.17 Error statistics for T2m at 12 UTC. Left: bias (dashed lines) and standard deviations (solid lines). Right: RMSE and number of observations. Red: UERRA, blue: downscaled, green: analysis.

The added value of the downscaling and analysis compared to the original UERRA data is exemplified for the two meter temperature at 12 UTC in Figure 6.17. Plots for other hours can be found in Appendix B.

The left panel shows time series of bias and standard deviation for the differences between model fields and the observations. Hence, the negative bias of the UERRA forecast (dashed red line) valid at 12 UTC means that it is generally too cold. Here, the downscaling improves on both the bias (dashed blue line) and the standard deviation (solid blue line). As a result the total error in terms of the RMSE is also improved by the downscaling (solid blue line in right panel).

The statistics for other hours follow a similar pattern. However, at 00 UTC the downscaling increases an already positive bias even more. This is consistent with the systematic positive downscaling increments seen during the winter that was shown in Figure 6.1.

Ideally the bias of the first guess entering the optimal interpolation analysis should have zero bias. This is not the really the case here and the bias seems to grow towards the end of the time period. There is however a slight improvement in the standard deviation of the UERRA data over time (solid red line in the left panel). On the other hand, the added number of observations towards the end of the period (gray line in right panel) does not

lead to any significant improvement on the analysis error. The reasons behind these effects have not been investigated.

The bias of the analysis is close to zero (dashed green line in left panel) and the RMSE (solid green line in right panel) is improved significantly as compared to the first guess (the downscaled UERRA field, solid bule line in right panel).

6.6.2 Two meter dewpoint temperature

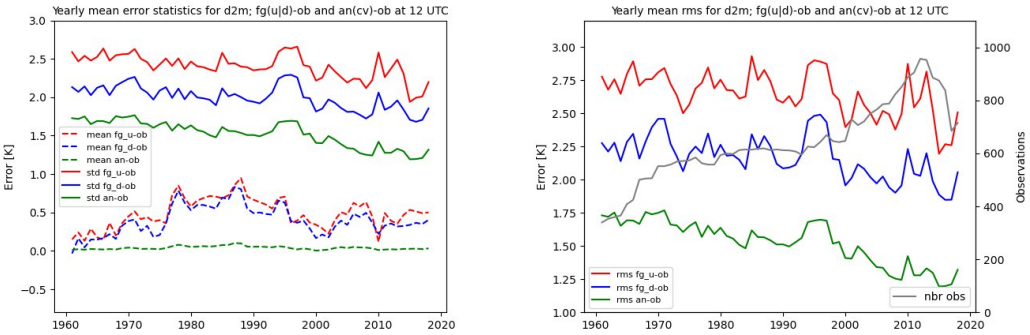

Figure 6.18 Error statistics for Td2m at 12 UTC. Left: bias (dashed lines) and standard deviations (solid lines). Right: RMSE and number of observations. Red: UERRA, blue: downscaled, green: analysis.

Figure 6.18 illustrates the time evolution of the bias, standard deviation, RMSE and number of observations for the two meter dew point temperature at 12 UTC (for plots valid at other hours, see Appendix B).

The downscaling (blue lines) improves the standard deviation but does not change the systematic overestimation of Td2m in the UERRA forecasts valid at 12 UTC. During the night (not shown here) the downscaling helps improving a negative bias at the end of the time period (although it overcompensates somewhat in the early years).

The number of observations increases over time (gray line in right panel) and this perhaps manifests itself in a slightly steeper slope of the RMSE for the analysis compared to the UERRA data (right panel).

The analysis looks good with zero mean and a distinct reduction of the RMSE compared to the first guess.

6.6.3 Two meter relative humidity

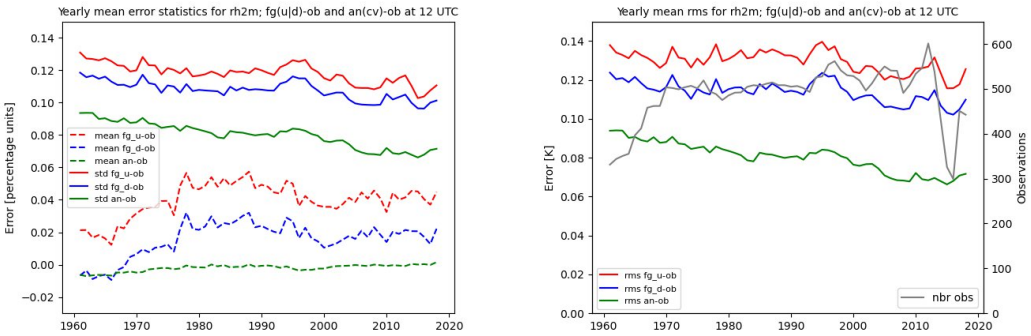

Figure 6.19 Error statistics for Rh2m at 12 UTC. Left: bias (dashed lines) and standard deviations (solid lines). Right: RMSE and number of observations. Red: UERRA, blue: downscaled, green: analysis.

An example of the error statistics for relative humidity at 12 UTC is given in Figure 6.19 (plots for other hours can be found in Appendix B). In this case, the downscaling is applied to T2m and Td2m from which Rh2m is diagnosed. Note that no observations of Rh2m enter the analysis. Instead the comparison is done to relative humidity values calculated from co-located observations of T2m and Td2m.

The downscaling clearly adds value compared to the UERRA forecasts (red lines in the left panel) of relative humidity, both in terms of lower bias and lower standard deviation (dashed and solid blue lines in the left panel). This in turn results in a lower RMSE (solid green line in right panel). However, the analysis cannot fully compensate for the bias in the first guess and one can see a small trend also in the bias of the analysis (dashed green line in the left panel).

6.6.4 Daily minimum temperature

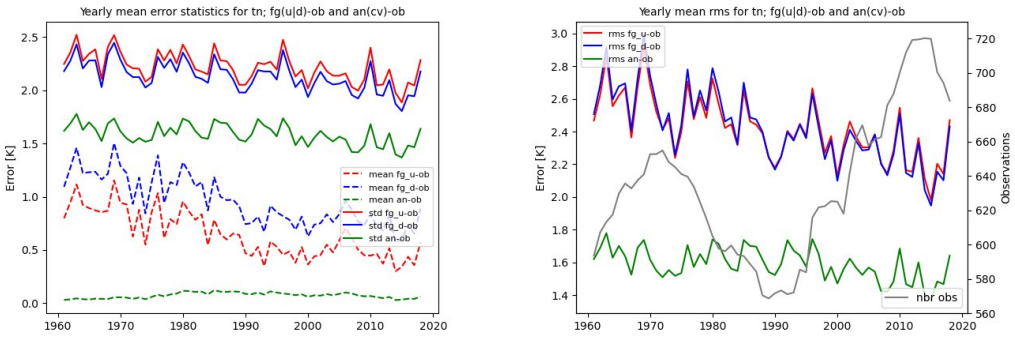

Figure 6.20 Error statistics for the daily minimum temperature. Left: bias (dashed lines) and standard deviations (solid lines). Right: RMSE and number of observations. Red: UERRA, blue: downscaled, green: analysis.

Time series with bias, standard deviation and RMSE for the daily minimum temperature is illustrated in Figure 6.20. Here the downscaling results in a slightly lower standard deviation but at the same time the positive bias is increasing. This is probably related to the way the downscaling increases the minimum temperatures during winter as seen in Figure 6.3. That modification of the UERRA fields is not beneficial since the analysis increments in Figure 6.13 shows that the analysis tries to compensate for this by systematically decreasing the minimum temperatures. The explanation is that the downscaling tries to mimic the MEPS forecast and it seems as if those are providing too high values for the daily minimum temperatures.

Anyway, the total error in terms of the RMSE is at least not worse than that of the original UERRA forecast. Hence at least no harm is done by applying the downscaling also for this parameter.

Note that there is a trend towards lower RMSE values over time for the first guess. This trend is not carried over to the analysis to the same extent, even though it should be further strengthened by the increase in observations towards the end of the period. The reason for this has not been investigated.

6.6.5 Daily maximum temperature

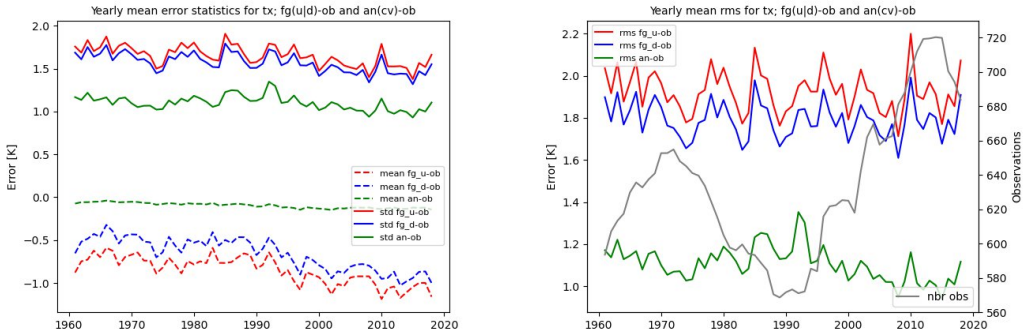

Figure 6.21 Error statistics for the daily maximum temperature. Left: bias (dashed lines) and standard deviations (solid lines). Right: RMSE and number of observations. Red: UERRA, blue: downscaled, green: analysis.

Figure 6.21 shows the error statistic in terms of bias, standard deviation and RMSE for the daily maximum temperature. The downscaling procedure results in a small improvement, both with respect to bias and standard deviation (blue lines in the left panel).

The negative bias in the first guess (dashed blue line in left panel) violates the assumption of zero bias for the optimal interpolation and is not fully eliminated by the analysis (dashed green line in left panel).

Note that the dip in the number of available observation around the 1980s and 1990s seems to be reflected in the RMSE of the analysis (green line in the right panel). Also note that the trend towards lower RMSE values that was seen for the daily minimum is not that pronounced for the daily maximum.

6.6.6 Daily precipitation

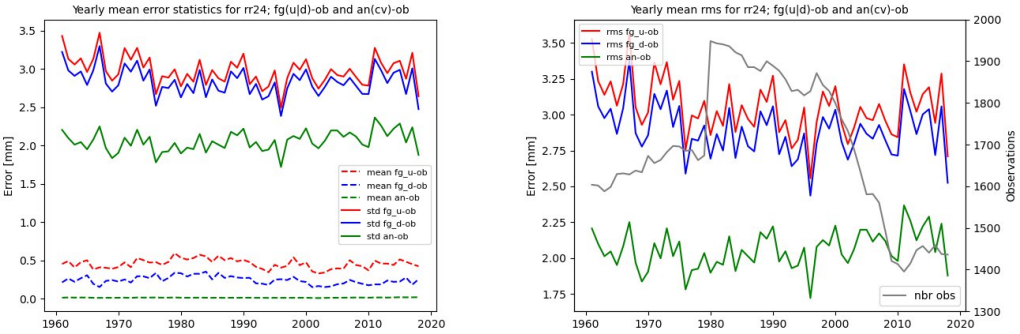

Figure 6.22 Error statistics for the daily precipitation. Left: bias (dashed lines) and standard deviations (solid lines). Right: RMSE and number of observations. Red: UERRA, blue: downscaled, green: analysis

Error statistics for the daily precipitation is depicted in Figure 6.22. The downscaling of the UERRA forecasts results in lower standard deviation (sold blue line in the left panel) as well as significantly lower bias (dashed blue line in the left panel).

The number of observations regarding the daily precipitation peaks during the 1980s and 1990s. This coincides with an improved RMSE for the first guess (solid blue line in right panel) but is not seen clearly in the RMSE of the analysis (solid green line in right panel).

The analysis of daily precipitation shows a nice zero like bias and a distinct added value on top of the first guess.

6.6.7 Daily snow cover

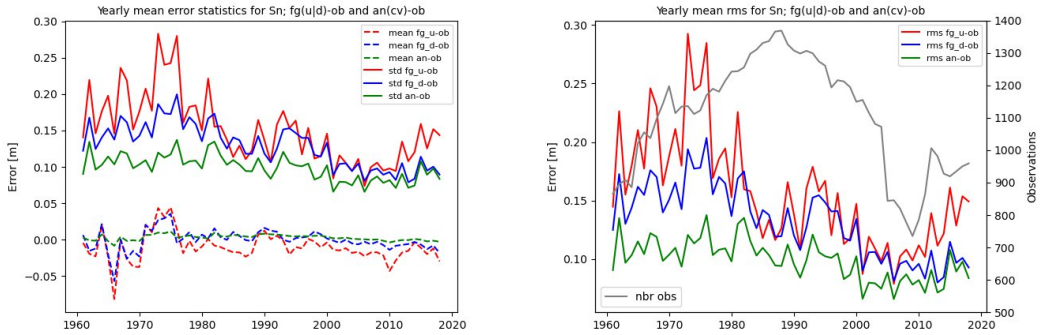

Figure 6.23 Error statistics for the daily snow cover . Left: bias (dashed lines) and standard deviations (solid lines). Right: RMSE and number of observations. Red: UERRA, blue: downscaled, green: analysis.

Figure 6.23 shows error statistics for the daily snow cover. The downscaling of the UERRA forecasts almost always results in lower standard deviation (sold blue line in the left panel) as well as a reduction in bias (dashed blue line in the left panel). There is no clear connection between the error in the first guess and the yearly mean snow depth (not shown), nor with its 95:th percentile. The reason behind the large errors in the UERRA snow fields during the 1970s has not been studied.

The increase in snow depth observations during the 1980s and 1990s (gray line in right panel) is similar to that shown for precipitation. Again there is no clear connection between the number of observations and the RMSE of the analysis (solid green line in right panel).

The analysis of daily snow cover shows almost zero bias and added value from the first guess, at least during the first and last 15 years. Without the quantile mapping the downscaling performs less well, especially during the first 15 years.

7 Conclusions

The effect of the downscaling was investigated by comparing its results with the original UERRA forecasts and the resulting output from the optimal interpolation was evaluated by means of cross validation and studies of analysis increments. The downscaling turned out to be adding value to all the variables with one exception. It increased the already positive bias of the UERRA forecasts for the night time two meter temperatures as well as the daily minimum temperatures.

Suitable parameters for the gridpp optimal interpolation were determined using a grid search with cross validation errors as the cost function. It turned out that the exact values of these parameters where not critical with respect to the analysis error. Because of the variable observation network it was however considered beneficial to let the parameters vary during the 58 year long time period.

Results from the study of the analysis increments showed significant systematic errors for the diurnal temperature and humidity cycles. Minimum temperatures in the downscaled first guess were too high and maximum temperatures too low causing the relative

humidity to be too high during the day and too low during the night. These effect where especially pronounced during winter daytime and summer nights. The common problem with NWP models forecasting precipitation too often also showed up here, resulting in a positive bias in the daily precipitation, especially over mountainous regions. The maps with analysis increments for humidity and precipitation showed some very localized features (notably along some coastal areas) that probably are associated with stations located at sites that do not represent the weather at the scale of the analysis.

The horizontal resolution of the SMHIGridClim data is 2.5 km but this is most probably not the effective resolution of the data. Even if the down scaling did a perfect job, the MEPS NWP model with its 2.5 km grid, probably have an effective resolution (i.e. the highest spatial resolution at which there is any meaningful information about the variable) that is about a magnitude coarser. This also means that the results from the evaluation of the analysis increments not necessarily show that the UERRA model actually has systematic errors, e.g. for the min and max temperatures. In order to make such claims, one would have to compare the UERRA output with observations on a scale matching its effective resolution.

Based on the results from the evaluation of the analysis we conclude that the SMHIGridClim data constitutes a reasonable description of the evolution of the studied variables in the Nordic countries (better in Sweden) for the time period 1961 - 2018. The cross validation results for hourly T2m for example are similar to what was found for the seNorge v2.0 and seNorge 2018 dataset regarding temperature (Lussana et al., 2016 and Lussana et al., 2019) as shown in Table 7.1. Note that the error regarding RR for the seNorge data only refers to cases where RR > 0.1 mm while the error for the SMHI dataset includes all cases. Still there is a good fit at the lower end of the interval suggesting that they are of similar quality. Also the error figures reported for the dataset FMI_ClimGrid (Aalto et al,, 2016) is of the same magnitude as shown in the same table. Note that it is more difficult to model temperatures and precipitation (rain as well as snow) in Norway (and Sweden) than in Finland where the orography is not as challenging.

	T2m	**Tn winter**	**Tn summer**	**Tx winter**	**Tx summer**	**RR**	**Sn**
SMHIGridClim	1.2 - 1.5 K	1.4 - 1.8 K		1.0 - 1.2 K		ca 2 mm	11cm
seNorge2.0/2018	1.0 - 1.4 K	2.0 - 4.0 K	1.5 - 1.8 K	1.0 - 2.5 K	1.0 - 1.5 K	2 - 6 mm	NA
FMI_ClimGrid	NA	1.0 - 1.7 K		0.5 - 0.8 K		0.4 - 1.5 mm	6.3 cm

Table 7.1 Mean RMSE for T2m (hourly), Tn, Tx, RR and Sn for three different gridded Nordic datasets.

8 User guidelines

In this section we aim to provide some background information and advice regarding best practices with the hope that users of the SMHIGridClim data should be able to make the most out of the data.

Metadata for SMHIGridClim	
Parameters, [units]	Temperature at 2m [K] Daily maximum temperature at 2m [K] Daily minimum temperature at 2m [K] Relative humidity at 2m [%] Daily Precipitation [kg m^{-2} s^{-1}] Snow depth [m] Surface Altitude [m] Land Area Fraction [%]
Horisontal resolution	2.5 km
Horisontal coverage	The data grid cover the Nordic countries: Sweden, Norway, Finland and Denmark, as illustrated in figure 2.1. In gridpoints outside these countries the amount of observations for the analysis was limited, which results in that some parts of the grid is only represented by the downscaled forecast from UERRA. Check appendix A on observations for details.
Vertical resolution	One level only
Temporal coverage	1961-01-01 to 2018-12-31
Temporal resolution	For temperature and relative humidity, the timestamp of the analyses differ depending on data period, as a result of the availability of surface observations for the analyses. 1961-1967 : analyses at 00, 06, 12, 18 UTC 1968-1996: analyses at 00, 03, 06, 09, 12, 15, 18, 21 UTC 1997- 2018: analyses at every hour For the remaining parameters, the resolution is daily at the following hours. Precipitation: 06 - 06 UTC Snow depth: 06 UTC Maximum temperature: 18-18 UTC Minimum temperature: 18-18 UTC
Data type and format	File format is Netcdf (NETCDF4_CLASSIC data model, file format HDF5) Metadata follows the convention CF-1.7
Grid	Projection: lambert conformal conic Projection parameters: earth radius = 6371229, false easting = 0, false northing = 0, latitude of projection origin = 63, longitude of central meridian = 15, longitude of prime meridian = 0, standard parallel = 63

Table 8.1 Data description for SMHIGridClim.

8.1 Data format description

Table 8.1 gives an overview of the dataset, with regards to available parameters, data coverage and description of the grid. More metadata information can be extracted from the netcdf datafiles.

8.2 Interpreting trends

Gridded datasets, without or with information from weather prediction models like SMHIGridClim, are what we have to rely on in order to map patterns related to climate trends. However, a word or two of caution is appropriate. Since the dataset is based on forecasts from the UERRA reanalysis topped with surface observations it is easy to view it as a perfect tool to establish climate trends. However, one should bear in mind that even if the UERRA reanalysis is based on a frozen model system (no model changes during the historical time period) the underlying observation network is not constant. The observations change in spatial distribution patterns, numbers and quality. Hence, even if we don't use the UERRA analysis data but the forecasts, they too are affected by the quality of the analysis. The same concern is valid for the observations used in our analysis. They also undergo, sometimes dramatic, changes in spatial and temporal patterns. Moreover, the parameters of the analysis procedure change with time in order to make the most out of the information from the variable observation network (with the exception of those for the daily precipitation). This could lead to artifacts in the data that are not to be attributed to climate change. Even if one tries to leave out model variations (like the time dependent gridpp parameters) and just use observations there is still the problem of stations coming and going. One resolution would be to only use the sites that are present throughout the whole time period but that would dramatically limit the information available for the analysis.

8.3 Variations in data quality

The two meter temperature and relative humidity are available with different time resolutions during different time periods. Analyses at 00, 06, 12 and 18 UTC are available for the entire time period, 1961 - 2018. These are complimented with analyses at 03, 09, 15 and 21 UTC from 1968 - 2018. Finally hourly analyses are available from 1997 onwards. As a rule of thumb there are more observations available at the 6 hourly cycles, followed by the 3 hourly and then the hourly. Another guideline is that the number of observations tends to be lower during the early years and then increase over time. However, there are exceptions and one should check out the time series plots for the cross validation data (includes the number of available observations) in Appendix B to make sure that there are not any dramatic changes that may affect the study at hand. Note that the difference in time resolution throughout the years can affect things like calculations of the daily mean temperature. The data is organized in monthly files and if one uses programs like cdo to compute daily means these may end up being based on different numbers of analyses depending on which year one looks at.

The two meter temperature and relative humidity observations were retrieved both from national archives in Norway, Sweden and Finland as well as the MARS archive at ECMWF adding information also for other countries covered by the SMHIGridClim grid. However, for the daily minimum and maximum temperatures and daily precipitation only national data was available. This means that the quality of the analysis differs significantly between these three Nordic countries and other areas, especially for the daily data (the quality of the sub daily data is probably better for the national archives compared to the MARS archive). Note that the results are probably most reliable for Sweden. Here we had best knowledge of the observations and there are less problems with steep topography and fractal coastlines like in Norway.

The grid covers both water and land areas but the analyses are only to be trusted over land since the observations used were all made over land surfaces. Data for grid boxes with a

small fraction of water could still be relevant since the structure functions limit how information is spread from land to water areas. One exception is snow cover which should be trusted over land only since no information about the ice cover has been taken into consideration during its analysis. The user is referred to the land-sea mask for filtering out information given a minimum requirement on the fraction of land in the points under investigation.

8.4 Extreme events

Using the SMHIGridClim data for studies of extreme events may be problematic. The first guess for the minimum and maximum temperatures is based on forecasts of minimum and maximum temperatures during 12 time intervals throughout the day and that is good. However, these forecasts are from the coarser UERRA model. The downscaling is then done for each time interval which is also good. One should however bear in mind that the downscaling is static at 00 and 12 UTC and since it is based on linear regression it tries to make the best fit with the mean error as the target. Hence it will probably not be very good at catching the extreme situations with inversions and the like. Similar cautions should be taken when looking at extreme precipitation. Besides the cautions mentioned earlier, another factor enters the equation. The OI analysis assumes that the error follows a normal distribution but for the high precipitation interval this will no longer hold. There is also the problem with precipitation being an on-off event. There is one probability for no precipitation and there is another probability for precipitation that in turn is associated with the probability regarding its value. Combined, this results in the precipitation analysis being smeared out and losing information about the high end tail of the distribution. There are plans on doing tailored analyses for extreme precipitation as mentioned in the next section.

9 Discussion

This section presents discussions on how the current SMHIGridClim data could be improved by increasing its quality, the area extent or the time period covered.

9.1 Improving the quality of the analysis

The quality of the SMHIGridClim data was shown to be comparable to other Nordic climatological analysis datasets. However, also some weaknesses were identified.

First the number of observations outside Sweden, Norway and Finland could be increased. There is more data available from the E-OBS but work need to done in order to make sure that the measuring times are compatible with what is aimed for in SMHIGridClim. One could also think of redistributing observations that refer to other intervals than 06-06 for RR and 18-18 for Tn/Tx, e.g. based in hourly information from the first guess. How successful such an approach would be need to be investigated.

If the current analysis was to be complemented by another analysis that only covers the time period of the “remote sensing era” (e.g. 1980 onwards) one could think of improving the quality by adding remote sensing observations in terms of satellite and radar data.

The downscaling of the T2m was shown to result in a positive bias during the night and this is probably due to the MEPS forecasts being biased. Since the downscaling tries to mimic them it too will be biased. This problem could be tackled by finding other high resolution data without such bias. Unfortunately, the new Arctic regional reanalysis CARRA does not cover the entire SMHIGridClim area, otherwise that could have been an alternative. If the SMHIGridClim data is revisited using data from CERRA (see below) one could possibly find a match between CARRA data and MEPS data from a later time period where the T2m bias in MEPS could have been reduced. The analyses of

Td2m, Tn and Tx are also affected by the MEPS bias for T2m and would hence also benefit from establishing a better downscaling of T2m. Finally, another alternative would be to skip the downscaling and settle for the 5.5 km resolution in the CERRA Land data. Since the effective resolution is probably much coarser than this it may not impact the quality in any significant way. Adaptations to high resolution topography is always possible as a post processing stage. One could also think of using a dynamic vertical adaptation (possible capturing inversions) depending on the CERRA 3D profiles, like what was done in EURO4M.

The downscaling of the daily precipitation worked reasonably well but the analysis did not take into consideration the non-normal distribution of this parameter. This causes problems both for cases with zero and high precipitation. As noted before the problem with the on-off behavior of precipitation could be reduced with a two step approach where first the area where there is precipitation is analysed and a second step then provides an analysis of how much precipitation there was within the precipitation area from the first step. The analysis of extreme precipitation could be improved by transforming the variable, before the analysis, in order to make it more normally distributed at the high end, e.g. using a box-cox transformation. After the analysis the variable is then back-transformed in order to be interpreted as precipitation again. Another thing that could be tried is a quantile mapping, perhaps with a focus on the high precipitation values.

The analysis of the temperature related entities was used with time varying parameters for the gridpp OI analysis function. However, it turned out that analysis was rather insensitive to the exact values of these parameters. Since the changes in those parameters still could show up when looking at trends in the temperature data one could consider redoing the analysis with a fixed set of parameters tuned to provide the best possible performance during the entire time period.

10 Extension of SMHIGridClim

Analysis with gridpp depends on that there is both reanalysis fields for the first guess and surface observations with good quality available. Thus, an extension of the dataset with regards to time period, grid area and/or analyzed variables requires satisfying input data of both types. As an alternative for some variables it is more relevant to complement SMHIGridClim data with other data sources, it is beneficial if they are or can be transformed into the same grid area and resolution. Below are a number of alternatives and perspectives of future work.

10.1 Additional variables

The present dataset includes near-surface air temperature and near-surface relative humidity (1-6 hourly resolution), as well as daily near-surface maximum and minimum temperatures, precipitation and snow depth. Examples of other parameters of interest are wind, solar radiation and more detailed data for precipitation and its extremes. There are also an interest in data for other non-meteorological parameters such as ground frost, and hydrological/oceanographical data, to calculate climate indices.

Wind is a difficult variable despite the fact that there is both forecast fields and observations available, since wind observations often are only representative for the very local conditions where the stations are located. Here it is probably better to use forecast fields, like in the EURO4M reanalysis project (precursor to UERRA) where the wind was downscaled semi-dynamically from 22 km to 5.5 km horizontal resolution and a similar approach could be used here as well.

For solar radiation and clouds, there are too few surface observations to process with gridpp. Thus it is more relevant to have a methodology based on satellite data. At SMHI the STRÅNG model is available with data for northern Europe (covering the years 1999-present), where work is currently being done to improve the cloud modeling by implementing optical depth from satellite observations. There are also other solar radiation datasets available, e.g. based on satellite or reanalysis data. However, their horizontal resolution is coarser than the 2.5 km used for SMHIGridClim.

Non-meteorological parameters such as ground frost or hydrological or oceanographical parameters, needs to be provided from other models, directly or by processing of GridClim variables.

Instead of trying to improve a single analysis of daily precipitation one could also think of making an analysis dedicated to extreme precipitation based on variable transformations. Relaxing the requirement of providing a good analysis for all precipitation amounts it would probably be easier to find a good solution for the extreme case separately.

10.2 Extended time period

To extend the dataset beyond 2018, another first guess than downscaling UERRA-HARMONIE needs to be used, as UERRA-HARMONIE ends in July 2019. Presently CERRA/CERRA-Land is the strongest candidate, that starts in 1984 and extends to near real time.

Another possibility is to extend with data from the operational version of GriPP analysis that is being setup at SMHI as successor to the current MESAN system. The operational gridpp analysis will be performed on the MEPS grid and hence it will overlap the SMHIGridClim grid with the same projection and resolution. Possible drawbacks are that the gridpp OI-parameters as well as the underlying observation network will differ making it more difficult to investigate climate trends.

Data could also be extended backwards, using ERA-5 that starts back in 1950. However as there is already a lack of observations in the early 1960 where SMHIGridClim starts, it is uncertain if there are enough observations for the analysis to bring extra value.

10.3 Extended data region

The current version of SMHIGridClim covers a Nordic region as shown in Figure 2.1. The main difficulty regards to spatial coverage was to access observations within the time available for the project. In any future reanalysis it should be considered to extend the data region to widen the applicability of data. Fore instance as input to hydrological (covering catchment areas) and oceanographic models (covering relavant sea areas), in combination with additional parameters needed. However, in order to be of value for oceanographic applications remote sensing data is probably vital. In the current analysis, (almost) no information is added to areas covered by sea.

The method used for the first guess with downscaling using MEPS forecast is limited by the smaller area covered by MEPS, but on the other hand if CERRA-Land is used the horizontal resolution of 5.5 km might be sufficient.

More observations can be retrieved from the E-obs dataset from KNMI, where a good contact is already established. It would be of value to have a closer collaboration as we learned in the current project that good knowledge about the observation dataset are critical. Furthermore, if data is to be extended in time and geographical area, it would be relevant to look for collaborative efforts among for instance the Nordic institutes.

11 Acknowledgements

We thank Viivi Kallio-Myers (FMI) and Mariken Homleid (MET No) for the extraction and preparation of their national observations.We thank Christophe Sturm and Erik Engström for their work with data quality check and evaluation. We also acknowledge O. Tange for his powerful program GNU parallel (Tange, 2018) that made our computations feasible.

12 References

Aalto, J., Pirinen, P., and Jylhä, K. (2016), New gridded daily climatology of Finland: Permutation-based uncertainty estimates and temporal trends in climate, J. Geophys. Res. Atmos., 121, 3807– 3823, doi:10.1002/2015JD024651.

Barnes, S. L., 1973: Mesoscale objective map analysis using weighted time series observations. NOAA Tech. Memo. ERL NSSL-62, 60, pp., https://repository.library.noaa.gov/view/noaa/17647.

Båserud, L., Lussana, C., Nipen, T.N., Seierstad, I.A., Oram, L. and Aspelien, T., 2020. TITAN automatic spatial quality control of meteorological in-situ observations. *Advances in Science and Research*, *17*, 153-163. doi: 10.5194/asr-17-153-2020.

Danielson, J.J., and Gesch, D.B., 2011, Global multi-resolution terrain elevation data 2010 (GMTED2010): U.S. Geological Survey Open-File Report 2011–1073, 26 p.

Frogner, I-L, Singleton, AT, Køltzow, MØ, Andrae, U. Convection-permitting ensembles: Challenges related to their design and use. Q J R Meteorol Soc. 2019; 145 (Suppl. 1): 90– 106. https://doi.org/10.1002/qj.3525

Gandin, L. S., 1966, Objective analysis of meteorological fields. Translated from the Russian. Jerusalem (Israel Program for Scientific Translations), 1965. Pp. vi, 242: 53 Figures; 28 Tables. £4 1s. 0d. Q.J.R. Meteorol. Soc., 92: 447-447. https://doi.org/10.1002/qj.49709239320

Hersbach, H, Bell, B, Berrisford, P, et al. The ERA5 global reanalysis. Q J R Meteorol Soc. 2020; 146: 1999– 2049. https://doi.org/10.1002/qj.3803

Klein Tank, A.M.G. and Coauthors, 2002. Daily dataset of 20th-century surface air temperature and precipitation series for the European Climate Assessment. Int. J. of Climatol., 22, 1441-1453. Data and metadata available at https://www.ecad.eu

Lussana, C., Uboldi, F. and Salvati, M.R., 2010. A spatial consistency test for surface observations from mesoscale meteorological networks. *Quarterly Journal of the Royal Meteorological Society, 136(649), 1075-1088. doi: 10.1002/qj.622.*

Lussana, C., Tveito, O. E., and Uboldi, F.: seNorge v2.0, Temperature. MET report No. 14/2016 ISSN 2387-4201 Climate, https://www.met.no/publikasjoner/met-report/met-report-2016/_/attachment/download/243074f4-09bf-4f63-b98a-f329b3661ce4:c586d2b116d185dc2ac000a1eca6cd98f2f5bdbd/MET-report-14-2016.pdf (accessed 12 April, 2021).

Lussana, C., Tveito, O. E., Dobler, A., and Tunheim, K.: seNorge_2018, daily precipitation, and temperature datasets over Norway, Earth Syst. Sci. Data, 11, 1531–1551, https://doi.org/10.5194/essd-11-1531-2019, 2019.

Panofsky, H. W. and Brier, G. W.: Some Applications of Statistics to Meteorology, The Pennsylvania State University Press, Philadelphia, 1968.

Tange, O. GNU Parallel 2018, March 2018, https://doi.org/10.5281/zenodo.1146014.

Themeßl, M. J., Gobiet, A., and Heinrich, G.: Empirical-statistical downscaling and error correction of regional climate models and its impact on the climate change signal, Climatic Change, 112, 449–468, doi:10.1007/s10584-011-0224-4, 2012.

UERRA,Copernicus Climate Change Service (C3S) (2020): UERRA regional reanalysis for Europe on single levels from 1961 to present. Copernicus Climate Change Service Climate Data Store (CDS), date of access October 2020 https://cds.climate.copernicus.eu/cdsapp#!/dataset/reanalysis-uerra-europe-single-levels?tab=overview

13 List of Appendices

Appendix A: Observations

Appendix B: Error statistics

Appendix C: Documentation of scripts

SMHI Publications

SMHI publishes seven report series. Three of these, the R-series, are intended for international readers and are in most cases written in English. For the others the Swedish language is used.

Names of the Series Published since
RMK (Report Meteorology and Climatology) 1974
RH (Report Hydrology) 1990
RO (Report Oceanography) 1986
METEOROLOGI 1985
HYDROLOGI 1985
OCEANOGRAFI 1985
KLIMATOLOGI 2009

Earlier issues published in serie RMK

1 Thompson, T. Udin, I. and Omstedt, A. (1974)
Sea surface temperatures in waters surrounding Sweden

2 Bodin, S. (1974)
Development on an unsteady atmospheric boundary layer model

3 Moen, L. (1975)
A multi-level quasi-geostrophic model for short range weather predictions

4 Holmström, I. (1976)
Optimization of atmospheric models

5 Collins, W.G. (1976)
A parameterization model for calculation of vertical fluxes of momentum due to terrain induced gravity waves

6 Nyberg, A. (1976)
On transport of sulphur over the North Atlantic

7 Lundqvist, J-E. Udin, I. (1977)
Ice accretion on ships with special emphasis on Baltic conditions

8 Eriksson, B. (1977)
Den dagliga och årliga variationen av temperatur, fuktighet och vindhastighet vid några orter i Sverige

9 Holmström, I. and Stokes, J. (1978)
Statistical forecasting of sea level changes in the Baltic

10 Omstedt, A. and Sahlberg, J. (1978)
Some results from a joint Swedish-Finnish sea ice experiment, March, 1977

11 Haag, T. (1978)
Byggnadsindustrins väderberoende, seminarieuppsats i företagsekonomi, B-nivå

12 Eriksson, B. (1978)
Vegetationsperioden i Sverige beräknad från temperaturobservationer

13 Bodin, S. (1979)
En numerisk prognosmodell för det atmosfäriska gränsskiktet, grundad på den turbulenta energiekvationen

14 Eriksson, B. (1979)
Temperaturfluktuationer under senaste 100 åren

15 Udin, I. och Mattisson, I. (1979)
Havsis- och snöinformation ur datorbearbetade satellitdata - en modellstudie

16 Eriksson, B. (1979)
Statistisk analys av nederbördsdata. Del I. Arealnederbörd

17 Eriksson, B. (1980)
Statistisk analys av nederbördsdata. Del II. Frekvensanalys av månadsnederbörd

18 Eriksson, B. (1980)
Årsmedelvärden (1931-60) av nederbörd, avdunstning och avrinning

19 Omstedt, A. (1980)
A sensitivity analysis of steady, free floating ice

20 Persson, C. och Omstedt, G. (1980)
En modell för beräkning av luftföroreningars spridning och deposition på mesoskala.

21 Jansson, D. (1980)
Studier av temperaturinversioner och vertikal vindskjuvning vid Sundsvall-Härnösands flygplats

22 Sahlberg, J. and Törnevik, H. (1980)
A study of large scale cooling in the Bay of Bothnia

23 Ericson, K. and Hårsmar, P.-O. (1980)
Boundary layer measurements at Klockrike Oct 1977

24 Bringfelt, B. (1980)
A comparison of forest evapotranspiration determined by some independent methods

25 Bodin, S. and Fredriksson, U. (1980)
Uncertainty in wind forecasting for wind power networks

26 Eriksson, B. (1980)
Graddagsstatistik för Sverige

27 Eriksson, B.(1981)
Statistisk analys av nederbördsdata. Del III. 200-åriga nederbördsserier

28 Eriksson, B. (1981)
Den "potentiella" evapotranspirationen i Sverige

29 Pershagen, H. (1981)
Maximisnödjup i Sverige (perioden 1905-70)

30 Lönnqvist, O. (1981)
Nederbördsstatistik med praktiska tillämpningar
(Precipitation statistics with practical applications.)

31 Melgarejo, J.W. (1981)
Similarity theory and resistance laws for the atmospheric boundary layer

32 Liljas, E. (1981)
Analys av moln och nederbörd genom automatisk klassning av AVHRR-data

33 Ericson, K. (1982)
Atmospheric boundary layer field experiment in Sweden 1980, GOTEX II, part I

34 Schoeffler, P. (1982)
Dissipation, dispersion and stability of numerical schemes for advection and diffusion

35 Undén, P. (1982)
The Swedish Limited Area Model. Part A. Formulation

36 Bringfelt, B. (1982)
A forest evapotranspiration model using synoptic data

37 Omstedt, G. (1982)
Spridning av luftförorening från skorsten i konvektiva gränsskikt

38 Törnevik, H. (1982)
An aerobiological model for operational forecasts of pollen concentration in the air

39 Eriksson, B. (1982)
Data rörande Sveriges temperaturklimat.

40 Omstedt, G. (1984)
An operational air pollution model using routine meteorological data

41 Persson, C. and Funkquist, L. (1984)
Local scale plume model for nitrogen oxides. Model description

42 Gollvik, S. (1984)
Estimation of orographic precipitation by dynamical interpretation of synoptic model data

43 Lönnqvist, O. (1984)
Congression - A fast regression technique with a great number of functions of all predictors

44 Laurin, S. (1984)
Population exposure to SO and NO_x from different sources in Stockholm

45 Svensson, J. (1985)
Remote sensing of atmospheric temperature profiles by TIROS Operational Vertical Sounder

46 Eriksson, B. (1986)
Nederbörds- och humiditetsklimat i Sverige under vegetationsperioden

47 Taesler, R. (1986)
Köldperioden av olika längd och förekomst

48 Wu Zengmao (1986)
Numerical study of lake-land breeze over Lake Vättern, Sweden

49 Wu Zengmao (1986)
Numerical analysis of initialization procedure in a two-dimensional lake breeze model

50 Persson, C. (1986)
Local scale plume model for nitrogen oxides. Verification

51 Melgarejo, J.W. (1986)
An analytical model of the boundary layer above sloping terrain with an application to observations in Antarctica

52 Bringfelt, B. (1986)
Test of a forest evapotranspiration model

53 Josefsson, W. (1986)
Solar ultraviolet radiation in Sweden

54 Dahlström, B. (1986)
Determination of areal precipitation for the Baltic Sea

55 Persson, C. Rodhe, H. and De Geer, L-E. (1986)
The Chernobyl accident - A meteorological analysis of how radionucleides reached Sweden

56 Persson, C. Robertson, L. Grennfelt, P. Kindbom, K. Lövblad, G. Svanberg, P.-A. (1987)
Luftföroreningsepisoden över södra Sverige 2 - 4 februari 1987

57 Omstedt, G. (1988)
An operational air pollution model

58 Alexandersson, H. and Eriksson, B. (1989)
Climate fluctuations in Sweden 1860 - 1987

59 Eriksson, B. (1989)
Snödjupsförhållanden i Sverige - Säsongerna 1950/51 - 1979/80

60 Omstedt, G. and Szegö, J. (1990)
Människors exponering för luftföroreningar

61 Mueller, L. Robertson, L. Andersson, E. and Gustafsson, N. (1990)
Mesoscale objective analysis of near surface temperature, humidity and wind. And its application in air pollution modelling

62 Andersson, T. and Mattisson, I. (1991)
A field test of thermometer screens

63 Alexandersson, H. Gollvik, S. and Meuller, L. (1991)
An energy balance model for prediction of surface temperatures

64 Alexandersson, H. and Dahlström, B. (1992)
Future climate in the Nordic region - survey and synthesis for the next century

65 Persson, C. Langner, J. and Robertson, L. (1994)
Regional spridningsmodell för Göteborgs och Bohus, Hallands och Älvsborgs län. A mesoscale air pollution dispersion model for the Swedish west-coast region
(In Swedish with captions also in English)

66 Karlsson, K.-G. (1994)
Satellite-estimated cloudiness from NOAA AVHRR data in the Nordic area during 1993

67 Karlsson, K-G. (1996)
Cloud classifications with the SCANDIA model

68 Persson, C. and Ullerstig, A. (1996)
Model calculations of dispersion of lindane over Europe. Pilot study with comparisons to measurements around the Baltic Sea and the Kattegatt

69 Langner, J. Persson, C. Robertson, L. and Ullerstig, A. (1996)
Air pollution Assessment Study Using the MATCH Modelling System. Application to sulphur and nitrogen compounds over Sweden 1994

70 Robertson, L. Langner, J. and Engardt, M. (1996)
MATCH - Meso-scale Atmospheric Transport and Chemistry modelling system

71 Josefsson, W. (1996)
Five years of solar UV-radiation monitoring in Sweden

72 Persson, C. Ullerstig, A. Robertson, L. Kindbom, K. and Sjöberg, K. (1996)
The Swedish Precipitation Chemistry Network. Studies in network design using the MATCH modelling system and statistical methods

73 Robertson, L. (1996)
Modelling of anthropogenic sulphur deposition to the African and South American continents

74 Josefsson, W. (1996)
Solar UV-radiation monitoring 1996

75 Häggmark, L. Ivarsson, K.-I. Olofsson, P.-O. (1997)
MESAN - Mesoskalig analys

76 Bringfelt, B. Backström, H. Kindell, S. Omstedt, G. Persson, C. and Ullerstig, A. (1997)
Calculations of PM-10 concentrations in Swedish cities- Modelling of inhalable particles

77 Gollvik, S. (1997)
The Teleflood project, estimation of precipitation over drainage basins

78 Persson, C. and Ullerstig, A. (1997)
Regional luftmiljöanalys för Västmanlands län baserad på MATCH modell-beräkningar och mätdata - Analys av 1994 års data

79 Josefsson, W. and Karlsson, J.-E. (1997)
Measurements of total ozone 1994-1996

80 Rummukainen, M. (1997)
Methods for statistical downscaling of GCM simulations

81 Persson, T. (1997)
Solar irradiance modelling using satellite retrieved cloudiness - A pilot study

82 Langner, J. Bergström, R. and Pleijel, K. (1998)
European scale modelling of sulfur, oxidized nitrogen and photochemical oxidants. Model development and evaluation for the 1994 growing season

83 Rummukainen, M. Räisänen, J. Ullerstig, A. Bringfelt, B. Hansson, U. Graham, P. and Willén, U. (1998)
RCA - Rossby Centre regional Atmospheric climate model: model description and results from the first multi-year simulation

84 Räisänen, J. and Doescher, R. (1998)
Simulation of present-day climate in Northern Europe in the HadCM2 OAGCM

85 Räisänen, J. Rummukainen, M. Ullerstig, A. Bringfelt, B. Hansson, U. and Willén. U. (1999)
The First Rossby Centre Regional Climate Scenario - Dynamical Downscaling of CO_2-induced Climate Change in the HadCM2 GCM

86 Rummukainen, M. (1999)
On the Climate Change debate

87 Räisänen, J. (2000)
CO_2-induced climate change in northern Europe: comparison of 12 CMIP2 experiments

88 Engardt, M. (2000)
Sulphur simulations for East Asia using the MATCH model with meteorological data from ECMWF

89 Persson, T. (2000)
Measurements of Solar Radiation in Sweden 1983-1998

90 Michelson, D. B. Andersson, T. Koistinen, J. Collier, C. G. Riedl, J. Szturc, J. Gjertsen, U. Nielsen, A. and Overgaard, S. (2000)
BALTEX Radar Data Centre Products and their Methodologies

91 Josefsson, W. (2000)
Measurements of total ozone 1997 – 1999

92 Andersson, T. (2000)
Boundary clear air echoes in southern Sweden

93 Andersson, T. (2000)
Using the Sun to check some weather radar parameters

94 Rummukainen, M. Bergström, S. Källén, E. Moen, L. Rodhe, J. and Tjernström, M. (2000)
SWECLIM – The First Three Years

95 Meier, H. E. M. (2001)
The first Rossby Centre regional climate scenario for the Baltic Sea using a 3D coupled ice-ocean model

96 Landelius, T. Josefsson, W. and Persson, T. (2001)
A system for modelling solar radiation parameters with mesoscale spatial resolution

97 Karlsson, K.-G. (2001)
A NOAA AVHRR cloud climatology over Scandinavia covering the period 1991-2000

98 Bringfelt, B. Räisänen, J. Gollvik, S. Lindström, G. Graham, P. and Ullerstig, A. (2001)
The land surface treatment for the Rossby Centre Regional Atmospheric Climate Model - version 2 (RCA2)

99 Kauker, F. and Meier, H E M. (2002)
Reconstructing atmospheric surface data for the period 1902-1998 to force a coupled ocean-sea ice model of the Baltic Sea

100 Klein, T. Bergström, R. and Persson, C. (2002)
Parameterization of dry deposition in MATCH

101 Räisänen, J. Hansson, U. Ullerstig A. Doescher, R. Graham, L. P. Jones, C. Meier, M. Samuelsson, P. and Willén, U. (2003)
GCM driven simulations of recent and future climate with the Rossby Centre coupled atmosphere - Baltic Sea regional climate model RCAO

102 Tjernström, M. Rummukainen, M. Bergström, S. Rodhe, J. and Persson, G. (2003)
Klimatmodellering och klimatscenarier ur SWECLIMs perspektiv

103 Segersson, D. (2003)
Numerical Quantification of Driving Rain on Buildings

104 Rummukainen, M. and the SWECLIM participants (2003)
The Swedish regional climate modelling program 1996-2003 Final report

105 Robertson, L. (2004)
Extended back-trajectories by means of adjoint equations

106 Rummukainen, M. Bergström S. Persson G. Ressner, E. (2005)
Anpassningar till klimatförändringar

107 Will not be published

108 Kjellström, E. Bärring, L. Gollvik, S. Hansson, U. Jones, C. Samuelsson, P. Rummukainen, M. Ullerstig, A. Willén, U. Wyser, K. (2005)
A 140-year simulation of European climate with the new version of the Rossby Centre regional atmospheric climate model (RCA3)

109 Meier, H.E.M. Andréasson, J. Broman, B. Graham, L. P. Kjellström, E. Persson, G. and Viehhauser, M. (2006)
Climate change scenario simulations of wind, sea level, and river discharge in the Baltic Sea and Lake Mälaren region – a dynamical downscaling approach from global to local scales

110 Wyser, K. Rummukainen, M. Strandberg, G. (2006)
Nordic regionalisation of a greenhouse-gas stabilisation scenario

111 Persson, G. Bärring, L. Kjellström, E. Strandberg G. Rummukainen, M. (2007).
Climate indices for vulnerability assessments

112 Jansson, A. Persson, Ch. Strandberg, G. (2007)2D meso-scale re-analysis of precipitation, perature and wind over Europe -ERAMESAN

113 Lind, P. Kjellström, E. (2008)
Temperature and Precipitation changes in Sweden; a wide range of model-based projections for the 21st century

114 Klein, T. Karlsson, P-E. Andersson, S. Engardt, M. Sjöberg, K. (2011)
Assessing and improving the Swedish forecast and information capabilities for ground-level ozone

115 Andersson, C. Bergström, R. Bennet, C. Thomas, M. Robertson, L. SMHI. Kokkola, H. Korhonen, H. Lehtinen, K. FMI (2013)
MATCH-SALSA Multi-scale Atmospheric Transport and Chemistry model coupled to the SALSA aerosol microphysics model

116 Strandberg, G. Bärring, L. Hansson, U. Jansson, C. Jones, C. Kjellström, E. Kolax, M. Kupiainen, M. Nikulin, G. Samuelsson, P. Ullerstig, A. and Wang, S. (2014)
CORDEX scenarios for Europe from the Rossby Centre regional climate model RCA4

117 Lennart Bengtsson, Nils Gustafsson1), Bo Döös2), Daniel Söderman, Lars Moen3), Thomas Thompson4), Paul Jakobsson, Gunnar Bleckert, Ann-Beate Henriksson, Bo Lindgren5) and Per Kållberg
1)Correspondig author, e-mail: Nils.Gustafsson@smhi.se
2)Deceased 2010 3)Deceased 2006
4)Deceased 2015 5)Deceased 2005
The Meteorological Auto Code (MAC) and Numerical Weather Prediction (NWP) at SMHI

Empty page

SMHI

Swedish Meteorological and Hydrological Institute
SE 601 76 NORRKÖPING
Phone +46 11-495 80 00 Telefax +46 11-495 80 01

ISSN: 0347-2116